2016

Substrate Specificity of the LipN Hydrolase from Mycobacterium ulcerans

Stephanie Raynor
Butler University, sraynor@butler.edu

BUTLER UNIVERSITY HONORS PROGRAM

Honors Thesis Certification

Please type all information in this section:

Applicant Stephanie Nicole Raynor
(Name as it is to appear on diploma)

Thesis title Substrate Specificity of the LipN Hydrolase from *Mycobacterium ulcerans*

Intended date of commencement 7 May 2016

Read, approved, and signed by:

Thesis adviser(s) Geoffrey C. Hoops 5/2/16
Date

Reader(s) [signature] 5/2/16
Date
Date

Certified by [signature] 5/2/16
Director, Honors Program Date

For Honors Program use:

Level of Honors conferred: University

Departmental

Substrate Specificity of the LipN Hydrolase from *Mycobacterium ulcerans*

A Thesis

Presented to the Department of Chemistry

College of Liberal Arts and Sciences

and

The Honors Program

of

Butler University

In Partial Fulfillment of the Requirements for

Graduation Honors

Stephanie Nicole Raynor

March 14, 2016

Dedication

This thesis is dedicated to my parents and friends, especially my mother, Sandra Raynor. I would also like to thank my research adviser Dr. Geoffrey Hoops and Dr. Jeremy Johnson for their guidance and support.

Acknowledgements

I would like to acknowledge Dr. Geoffrey Hoops and Dr. Jeremy Johnson for the time, guidance, and support they have given me to make this thesis possible.

The Department of Chemistry for their resources and support.

The Butler University Honors Program for their assistance and support.

Butler Summer Institute

Indiana Academy of Sciences

Dr. Luke Lavis at The Howard Hughes Medical Institute for synthesizing some of the Fluorogenic substrates used in this study.

Table of Contents

Abstract

Mycobacterium ulcerans is the causative agent of Buruli ulcer, a tropical skin disease that affects thousands of individuals annually. Recent studies have revealed that lipolytic enzymes are involved in the pathogenicity processes of mycobacterium and could be potential targets for novel antibiotics. LipN is one proposed serine hydrolase in *Mycobacterium ulcerans* that contains the conserved α/β hydrolase protein fold and utilizes the conserved catalytic traid of serine, histidine, and aspartate/glutamate. The physiological substrate and biological role of LipN from *M. ulcerans* have not yet been determined. In this study, LipN was cloned into a pET28a plasmid and overexpressed in an *E. coli* host. Ni-affinity chromatography was used to purity LipN from the *E. coli* host cell lysate. The substrate specificity of LipN was elucidated using enzymatic assays utilizing a library of 15 latent fluorophore substrates. Steady state kinetic data was fit to the Michaelis-Menten equation; k_{cat}, K_M, k_{cat}/K_M were derived to quantitate the structure-activity relationships that provide insight into the substrate specificity of LipN. The LipN protein showed preference for 2-4 carbon chains with the highest catalytic efficiency (k_{cat}/K_M of 881±64 $M^{-1}s^{-1}$) for an alky ether ester substrate.

Introduction

Background and Literature Review

Mycobacterium ulcerans (*M. ulcerans*) is the bacterium responsible for the infectious disease Buruli ulcer, which effects between 5,000-6,000 individuals annually[1]. Buruli ulcer is an ulcerative skin disease mainly targeting children under the age of 15 who live in Africa, South America, and the Western Pacific regions[1,2,3]. It is the third most common mycobacteriosis in humans after tuberculosis and leprosy[3]. Untreated, Buruli ulcer infection can lead to long-term functional disabilities or death. The method by which Buruli ulcer is transmitted remains poorly understood and there is currently no vaccination available; treatment is centered on early detection and combinations of broad range antibiotics (such as rifampicin and streptomycin)[1,2,3]. Unfortunately, many of the anti-mycobacterial drugs currently available do not inhibit latent mycobacteria or drug-resistant strains[1,4,5,].

Mycobacterial lipolytic enzymes and their involvement in the virulence and pathogenicity processes of mycobacterium have recently received attention[6,7,8]. Lipolytic enzymes are abundant in mycobacteria, where they mediate necessary cellular functions such as protein recycling, cell membrane synthesis, and signaling[6,7]. Thus, mycobacterial lipase enzymes appear to be viable drug targets[6,7,8]. Serine hydrolases are a class of lipase enzymes that share a common chemical mechanism; they hydrolyze a carboxylic ester to an alcohol and carboxylate using a catalytic triad of residues: serine, histidine, and aspartate/glutamate[6.7,9] (*Figure 1*). One proposed serine hydrolase in *Mycobacterium ulcerans* is LipN.

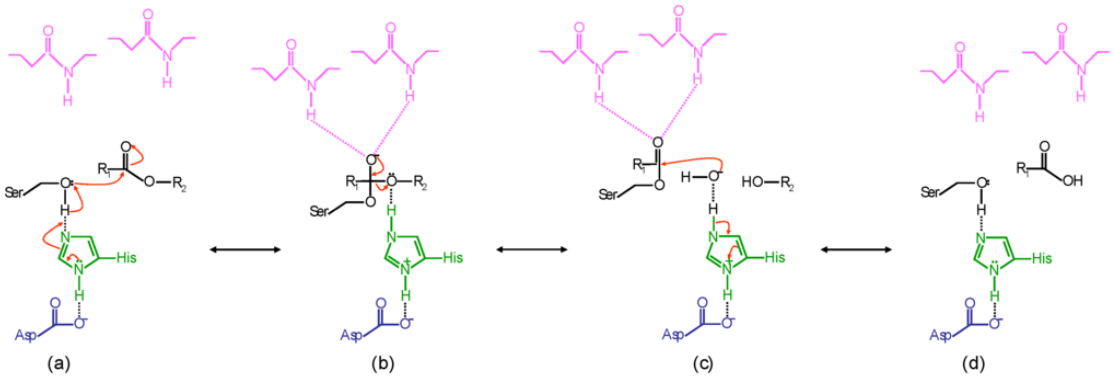

Figure 1: Serine hydrolases catalyze the hydrolysis of a carboxylic ester to an alcohol and carboxylate using a catalytic triad of residues: serine, histidine, and aspartate/glutamate. (a) an ester substrate enters the active site of the enzyme. The nucleophilic serine is activated by proton relay involving an acidic residue and a basic histidine residue. The activated serine residue attacks the carbonyl carbon of the ester substrate. (b) Formation of the tetrahedral intermediate followed by its collapse, releasing the alcohol product and forming an acyl-enzyme intermediate. (c) A nucleophilic water molecule attacks the carbonyl of the acyl-enzyme intermediate, forming a second tetrahedral intermediate. (d) The second tetrahedral intermediate collapse, releasing the carboxylic acid product and regenerating the nucleophilic serine[9,10].

The genome of *Mycobacterium ulcerans* has been sequenced[11] and includes a DNA sequence that codes for the LipN protein[14]. However, basic biochemical properties of the LipN enzyme from *M. ulcerans* have not been characterized and the three-dimensional structure has not been experimentally determined. The natural physiological substrate and biological role of the LipN enzyme are unknown.

Homologs of the LipN protein in other organisms have been identified and characterized. Of particular interest is the recent characterization of LipN (Rv2970c) of *Mycobacteria tuberculosis*[12]. Jadehi et al. characterized LipN (Rv2970c) of *M. tuberculosis* and its probable role in xenobiotic degradation. The enzyme showed

preference for short chain carbon substrates with no positional specificity and was inhibited with Tetrahydrolipstatin, RHC-80267, and N-bromosuccinimide (*Figure 2*). The active site residues were confirmed to be Ser216, Asp316, and His346 and the enzymatic activity was shown to be dependent on the non active site Trp145 residue. The LipN sequence of *M. tuberculosis* exhibited high identity (38%) with hHSL family enzymes and contains all the same conserved motifs. Jadehi et al. suggested that LipN from *M. tuberculosis* functions as an arylesterase in the bisphenol A degradation pathway, converting 4-HPS to hydroquinone[12] (*Figure 3*).

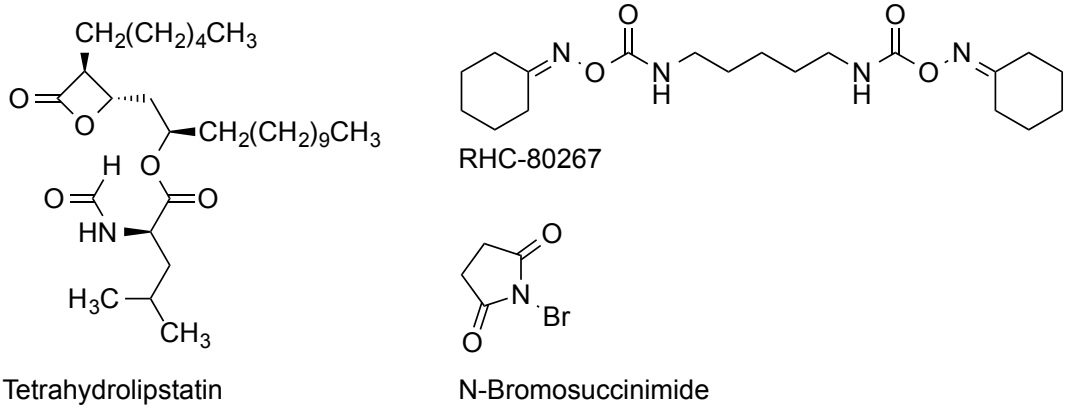

Figure 2: Chemical structures of the inhibitors Tetrahydrolipstatin, RHC-80267, and N-bromosuccinimide[12].

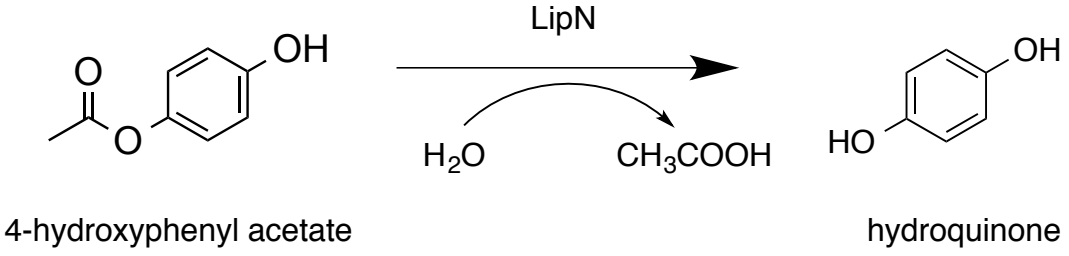

Figure 3: Proposed reaction scheme showing 4-hydroxyphenylacetate hydrolase activity of LipN from *Mycobacterium tuberculosis*[12].

BLAST sequence alignment revealed that the LipN protein from *M. ulcerans* shows high sequence identity (72%) to the LipN protein from *M. tuberculosis (Figure 4)*. Based on the sequence similarity, it can be predicted that the overall structure and active site of the two LipN proteins are quite alike. Therefore, characterizing LipN from *M. ulcerans* will provide structural insights for other mycobacterial lipolytic enzymes, especially other mycobacterial LipN proteins. On an applied scale, characterizing LipN from *M. ulcerans* could aid in the rational design of inhibitors targeting the LipN enzyme, and thus potential anti-mycobacterial drugs[13].

```
Query  22   MTNSLPGETDLHPETVHATMSWLSRVQNTVTVVGAKVIPWVPDVAKRLITRGRSVIIDGN  81
            MT SLPG  DL     H  M W  RVQ TV  VG KV+PW+P  AKR+++ GRSVIIDGN
Sbjct  32   MTKSLPGVADLRLGANHPRM-WTRRVQGTVVNVGVKVLPWIPTPAKRILSAGRSVIIDGN  90

Query  82   TLDPALQLMLSGMRVVGLDGLVIDDDLAASRAHMREAMLGFPGPQIHVDVEELTLPGPAG  141
            TLDP LQLMLS  R+ G+DGL +DDD+ ASRAHMR      PGPQIHVDV +L++PGPAG
Sbjct  91   TLDPTLQLMLSTSRIFGVDGLAVDDDIVASRAHMRAICEAMPGPQIHVDVTDLSIPGPAG  150

Query  142  DISARHYRPPGDAAAPLLVFYHGGGWALGDLDTHDAVCRLTCRDAGIHVLAIDYRLSPEH  201
            +I ARHYRP G  A PLLVFYHGGGW LGDLDTHDA+CRLTCRDA I VL+IDYRL+PEH
Sbjct  151  EIPARHYRPSGGGATPLLVFYHGGGWTLGDLDTHDALCRLTCRDADIQVLSIDYRLAPEH  210

Query  202  RAPAAIDDAFAAFEWAHAHAA-ELGALPGRVAVGGDSAGGNLAAVVSQLARDS----GGP  256
             APAA++DA+AAF WAH HA+ E GALPGRVAVGGDSAGGNL+AVV QLARD     GGP
Sbjct  211  PAPAAVEDAYAAFVWAHEHASDEFGALPGRVAVGGDSAGGNLSAVVCQLARDKARYEGGP  270

Query  257  APIFQWLIYPRTDFAGRTRSASLFARGFLLTKRDIDWFHSQYLKGSGIEPTDPRVSPLRA  316
             P+ QWL+YPRTDF  +TRS  LF  GFLLTKRDIDWFH+QYL+ S ++P DPR+SPL A
Sbjct  271  TPVLQWLLYPRTDFTAQTRSMGLFGNGFLLTKRDIDWFHTQYLRDSDVDPADPRLSPLLA  330

Query  317  ESLAGLAPALIAVAGFDPLRDEGENYATALRAAGTPVDLRAMGSLTHGFLNLFPLGGGCA  376
            ESL+GLAPALIAVAGFDPLRDEGE+YA ALRAAGT VDLR +GSLTHGFLNLF LGGG A
Sbjct  331  ESLSGLAPALIAVAGFDPLRDEGESYAKALRAAGTAVDLRYLGSLTHGFLNLFQLGGGSA  390

Query  377  AATSELISALRAHLTRV  393
            A T+ELISALRAHL+RV
Sbjct  391  AGTNELISALRAHLSRV  407
```

Figure 4: BLAST protein sequence alignment of the expressed amino acid sequence of LipN of *M. ulcerans*. Query sequence is LipN of *M. ulcerans* and subject sequence is LipN of *M. tuberculosis*; alignment is shown in between the query and subject sequence. There is a 72% identity between the two sequences.

Fortunately, the Seattle Structural Genomics Center for Infectious Disease has cloned LipN sequence from *M. ulcerans* into a plasmid vector containing a histidine tag as part of larger project aimed at identifying and characterizing biomedical relevant drug targets, enzymes, and virulence factors of infectious diseases[14].

Objective

My research aims to gain a better understanding of the substrate specificity of the serine hydrolase LipN from *M. ulcerans* by measuring its enzymatic activity using a library of latent fluorophore ester substrates.

Significance

No scientific articles focused on the characterization of LipN from *M. ulcerans* have been published, so all of my findings represent new contributions to the understanding of this enzyme. My research provides data of basic biochemical interest; clues to the identity of the physiological substrate and the biological role for the LipN enzyme in *M. ulcerans*. On a global scale, this data may contribute to the rational design of inhibitors targeting the LipN enzyme, and thus potential anti-mycobacterial drugs.

Central Methodology: Enzymatic Assays using Latent Fluorophore Substrates

A prerequisite to establishing an enzyme's true activities and physiological function is biochemical characterization using specific substrates[7]. An accurate enzymatic assay is essential for the analysis of the substrate specificity and binding affinity of an enzyme. The enzymatic assay employed in this study makes use of small

fluorescent molecular dyes as substrates to quantitate the kinetic activity of a given hydrolysis reaction.

Fluorescent dyes are invaluable tools for understanding biological processes, specifically, they facilitate studies of reaction kinetics and binding affinity[15]. These fluorescent compounds and their derivatives are useful as substrates for bacterial enzymes such as esterases and serine hydrolases based on their selective fluorescent properties[15,16,17].

The relative rate of hydrolysis of a series of fluorogenic ester substrates, as catalyzed by LipN, was the primary method by which I studied the structure-activity relationship that revealed clues to the substrate specificity of LipN. The hydrolysis reaction converts a non-fluorescent starting material into a fluorescent product, called fluorescein (*Figure 5A*)[16,17]. This reaction is negligibly slow in the absence of a catalyst[16,17]. The LipN enzyme catalyzes this hydrolysis reaction, so the rate of appearance of fluorescence is dependent upon the efficiency of catalysis by LipN. This basic hydrolysis reaction can be measured for various esters, whose structures share the same aromatic core but include variable acyl groups (*Figure 5B*)[16,17]. The reaction catalyzed by LipN was measured under steady state conditions, meaning the concentration of the substrate will be much higher than the concentration of the catalyst and only the initial reaction rate rather than the entire time course of the reaction was measured.

The previously synthesized Butler library of latent fluorophores was used to study the activity of LipN esterase in order to better understand the binding affinity of

the enzyme as well as potentially provide insight to the physiological role of the enzyme (*Figure 5*)[16,17,18,19,20].

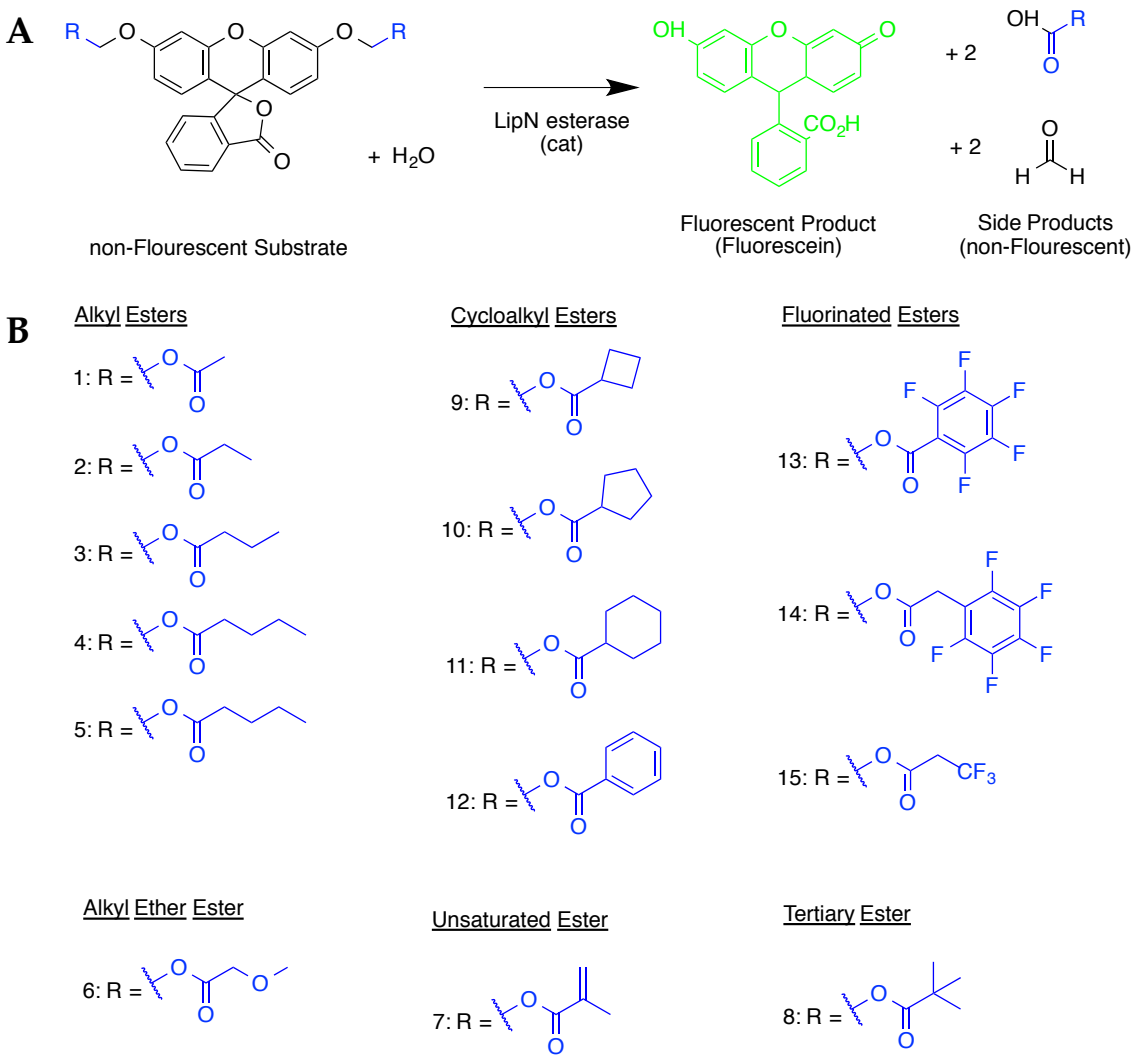

Figure 5: LipN catalyzed hydrolysis of various latent fluorogenic ester substrates. (A) Hydrolysis of the ester bond on the diacyloxymethyl ether fluorescein substrates by LipN converts the fluorescein core from the nonfluorescent lactone to the fluorescent quinoid form, fluorescein. (B) Fluorogenic substrate library of the 15 acyl R-groups. Each of the substrates has a diacyloxymethyl ether fluorescein core. The varying R-groups are organized based on chemical functionality. All of the substrates were synthesized as described previously.

Data analysis of Enzymatic Assays

As a common practice, the catalytic activity of enzymes is quantitated using two parameters: K_M and k_{cat}. K_M indicates the binding affinity of the substrate to the enzymatic protein and k_{cat} represents the maximum catalytic rate or in other words, the rate by which the substrate is converted to the product. The values of K_M and k_{cat} are dependent on the chemical identity of the fluorogenic substrate in the hydrolysis reaction (*figure 5*)[10,17,18,19,20]. The K_M and k_{cat} values are obtained by fitting the hyperbolic rate data to the Michaelis-Menten equation[10]:

$$\text{Observed steady state rate} = \frac{k_{cat} \times [\text{Enzyme}] \times [\text{substrate}]}{K_M + [\text{substrate}]}$$

Fitting the hyperbolic rate data to the Michaelis-Menten equation also gives V_{MAX}, which is the maximum rate at which the enzyme is saturated with substrate[9]. K_M is calculated by finding the substrate concentration at which V_{MAX} is at half of its value[9]. The efficiency at which LipN catalyzes the hydrolysis reaction was quantitated as the k_{cat}/K_M ratio to derive the global structural and functional relationship between LipN and the various acyl groups tested. The enzyme is expected to show preference for some acyl groups over others, and therefore catalyze reactions with variable efficiency depending on the specificity with which the enzyme binds the various substrates. Substrates that are more efficiently hydrolyzed by LipN are assumed to bear acyl groups that more closely resemble the true physiological substrate for the LipN enzyme in *M. ulcerans*[18,19,20].

Error Analysis of Enzymatic Assays

The error associated with the values for V_{MAX} and K_M were calculated using Origin Software based on the rate data fit to the hyperbolic Michaelis-Menten curve. The error for the k_{cat} and k_{cat}/K_M values were derived according to the following equations[10]:

$$k_{cat}\ \text{error} = \frac{V_{MAX}\ \text{error}}{[\text{Enzyme}]}$$

$$\frac{k_{cat}}{K_M}\ \text{error} = \frac{k_{cat}}{K_M}\left[\sqrt{\left(\frac{k_{cat}\ \text{error}}{k_{cat}}\right)^2 + \left(\frac{K_M\ \text{error}}{K_M}\right)^2}\right]$$

Materials and Methods

Molecular Cloning

The gene coding for LipN was previously cloned into an AVA0421 vector, which is a derivative of pET12b bacterial expression vector, by Seattle Structural Genomics Center for Infectious Disease (SSGCID)[14] but failed to properly overexpress. The LipN gene was removed from the AVA0421 vector and cloned into a pET28a plasmid® following the Novagen pET System Manual Protocol[21].

A double digest using the restriction endonucleases Xba1 and Xho1 was performed for AVA0421 and pET28 vectors in 37°C water bath for 2 hours. Samples were then placed in 65°C hot bath for 20 minutes to denature the restriction enzymes.

The ligation reaction of the double digested vectors (5µL) was performed with T4 ligase (2µL), ATP (2µL), and T4 ligase buffer (5µL) in a thermo cycler for 12 hours at 15°C.

Samples of the digest reaction (5µL) and undigested reaction (5µL) with 6X Gel-loading dye (5µL) were analyzed on 0.8% agarose gel run in Tris/Acetate/EDTA buffer (132V; 45min.) and stained with ethidium bromide for 15 min. The gel was visualized using a Proteinsimple FluoroChem Q imager.

Bacterial Transformation into the *E. coli* strain DH5α

An aliquot of the ligation mixture (10µL) was added to DH5α *E. coli* cells and incubated on ice for 30mins. The cells were heat shocked for 40 seconds in 42°C water bath and immediately placed back on ice for 2min. The transformed cells were transferred to a glass culture tube with 1mL of liquid LB media and shaken at 225 rpm for 1 hour at 37°C. The cells were then incubated at 37 °C overnight on LB-Kanamycin plates.

Miniprep

The LipN plasmid was purified from *E. coli* using an IBI High-Speed Plasmid Mini Kit[22]. Transformed *E. coli* cultures were centrifuged (16,000 x g; 1 min.) and the supernatant was discarded. The cell pellet was resuspended using PD1 Buffer, followed by vortexing (200 µL, buffer contains RNase). Bacterial cells were lysed (200 µl of PD2 Buffer) and incubated at room temperature until the lysate was homogenous (2 min). Cells were neutralized (300 µl of PD3 Buffer) and immediately inverted 10 times followed by centrifugation (16,000 x g; 3 min.). Supernatant, containing the plasmid DNA, was added to PD column and centrifuged (16,000 x g; 30 sec.). The column was washed (W1 Buffer; 400 µl) followed by centrifugation (16,000 x g; 30 sec.). Wash Buffer was added into PD column (600 µl) and centrifuged (16,000 x g; 30 sec.). The PD column and collection tube was centrifuged for 16,000 x g and 3 min. to remove

residual ethanol. Plasmid DNA attached to the DNA affinity column was incubated at room temperature for 5 min., and then eluted with 50µl ddH_2O followed by centrifugation (16,000 x g; 2 min.).

DNA Concentration

The DNA concentration of the purified plasmid was determined via ultraviolet absorption spectroscopy using a Synergy H1 Hybrid reader with a Take3 microplate and analyzed through Gen5 program (240-300nm). Four samples of 2 µL were analyzed with respect to water.

Sequence Analysis

Purified plasmid samples (10µL) of adequate DNA concentration were sent for sequencing at Genewiz. The T7 forward and T7 reverse primers were used to evaluate the LipN gene sequence. The results were examined using the Expasy translate program, protein BLAST, and BioEdit Sequence Alignment Editor. The Expasy translate program was used to convert DNA sequence to protein sequences, and protein BLAST was used to analyze the alignment of the protein sequence with the wild-type LipN sequence. The BioEdit Sequence Alignment Editor used both the reverse and forward sequences to reconstruct the full LipN gene and compare the LipN sequence in the pET28a plasmid to the wild-type LipN sequence.

Bacterial Transformation into *E. coli* strains BL21(DE3)RIPL and BL21(DE3)pLysS

The pET28a plasmid was transformed into the protein expression strains BL21(DE3)RIPL and BL21(DE3)pLysS of *E. coli.* The pET28a plasmid (3 µL) was added to BL21(DE3)RIPL and BL21(DE3)pLysS *E. coli* cells and incubated on ice for

30 mins. The cells were heat shocked for 40 seconds in 42 °C water bath and immediately placed back on ice for 2 min. The transformed cells were transferred to a glass culture tube with 1 mL of LB media and shaken at 225 rpm for 1 hour at 37 °C. The BL21(DE3)RIPL cells were then incubated at 37 °C overnight on LB-Kanamycin-Chloramphenicol plates and the BL21(DE3)pLysS on LB-Kanamycin plates.

IPTG Induced Overexpression of pET28a plasmid

Starter cultures of 5mL of LB-chloramphenicol-kanamycin for BL21(DE3)RIPL transformed cells and LB-Kanamycin for BL21(DE3)pLysS transformed cells were grown to saturation. The starter cultures were used to seed 250 mL cultures of LB with the appropriate antibiotics for both *E. coli* strains and grown to the optimum growth density of 0.8 with shaking at 225 rpm, 37 °C. Cultures were then cooled to 18°C and inducted with 250 µl of Isopropyl β-D-1thiogalactopyranoside (IPTG) and shaken overnight (225 rpm, 18°C). Cultures were then pelleted by centrifugation (16,000 x g, 10 mins, 4°C) and samples of 20 µl of both strains where taken to analyze the overexpression.

Protein Purification

The pelleted 250 mL cultures of both transformed *E. coli* strains were suspended in 3.0mL of 10X phosphate buffered saline solution (PBS) with 75 mg/mL of lysozyme and 800µL of 10X BugBuster. The solutions were placed on a rotor and lysed for 4 hours at 10°C. The lysed bacteria were centrifuged (16,000 x g, 5min) at 10 °C and a sample of the supernatant (40 µL) was transferred and stored for SDS-PAGE gel. The pellet was discarded. Nickel-NTA agarose resin (500 µL) was added to the remaining supernatant and the mixture was placed on the rotator (10 °C, for 45 min) to allow the

protein to bind to the nickel resin. The resin with protein bound was collected by centrifugation (2,000 x g, 2 min, 10 °C), and the flowthrough (40 µL) was saved for SDS-PAGE. The resin was resuspended and washed in PBS +10mM imidazole (3X at 1.5mL each) and then recollected through centrifugation (2,000 xg, 15sec, RT). The resin was then washed with increasing concentrations of imidazole (PBS + 25mM imidazole; 2X at 1.5 mL each and PBS + 50mM imidazole; 2X at 1.5 mL each) and samples were collected for SDS-PAGE after each initial wash. The bound LipN enzyme was eluted in 600 µL of PBS + 250 mM imidazole by allowing the solution to sit on ice for 10 min while being inverted every minute followed by centrifugation (16,000 x g, 1 min, 4 °C). Eluted protein (600 µL) was dialyzed in PBS buffer at 4 °C for two days.

SDS-PAGE

IPTG induced overexpression samples, protein purification samples, and purified LipN protein samples were analyzed using a pre-poured SDS-PAGE gel (4-20% gradient) and run at 180 V for 45 min in 1X tris-glycine buffer. Samples were prepared with 6X SDS loading dye and heated at 95°C for 10min to denature the proteins. The gel was stained with colloidal coomassie brilliant blue for 24 hr and destained for 24 hr before imaging.

Protein Concentration

The concentration of LipN in solution was quantitated by ultraviolet light absorption spectroscopy (Synergy H1 Hybrid reader with take3 microplate), using the theoretical extinction coefficient for LipN of $\Sigma_{280} = 4.2 \times 10^4\ M^{-1}cm^{-1}$ based upon its amino acid sequence. PBS dialysis buffer (2 µL) was used as the baseline for the UV reading. Protein samples of 2µL were analyzed in duplicates. The instrument utilizes the

Beer-Lambert equation to correlate the absorbance at 280 nm with the concentration of the protein based on the theoretical extinction coefficient.

Thermal Stability

The thermal stability of the protein was measured using differential scanning fluorimetry[23,24] at a concentration of 0.3mg/mL. The thermal stability samples were prepared in a 96 well plate by adding 3.33µl of LipN protein, 1µl of Sypro Orange dye, and 20.67µl of 1X PBS. Each sample was run in triplicate using the Bio-rad C1000 Thermocycler with CFX96 Real-time system which heats the samples from 15°C to 95°C at 1°C/min.

Enzyme Kinetics

Enzymatic activity of LipN was measured using Fluorogenic hydrolase substrates in a 96-well microplate assay. The fluorogenic substrates were synthesized as previously reported[16,17,18,20]. The substrates were stored as a 10 mM stock solution in DMSO and diluted with PBS containing acetylated BSA (0.1 mg/mL) to an initial concentrations of 100 µM. Eight serial dilutions were prepared for each substrate in triplicate using PBS-BSA (1:3; 60 µL into 180 µL total volume). Eight serial 1:2 dilutions of the fluorescein standard in PBS-BSA was prepared from a stock solution of 300nM of fluorescein in 10% DMSO. Substrate dilutions of 95 µL were then transferred to a black 96-well microplate. The LipN protein (5 µL of 300 µg/mL) was then added to the diluted Fluorogenic substrates to initiate the hydrolysis reaction (final protein concentration 15 µg/mL; final volume 100 µL). The fluorescence change (λ_{ex}= 485 nm, λ_{em}=520 nm) was measured using a Synergy H1 Hybrid fluorescent plate reader and then converted to molar concentrations using the standard fluorescein curve. The initial

rates of the hydrolysis reaction were plotted against the Fluorogenic substrate concentrations and then the saturation enzyme kinetic data was fit to a standard Michaelis-Menten equation using Origin software. The enzymatic activity of LipN with each substrate was calculated by the Michaelis-Menten values k_{cat}, K_M, and k_{cat}/K_M.

Results and Discussion

Molecular Cloning and Sequencing

The gene coding for LipN was previously cloned into pET14 plasmid but failed to properly overexpress. It was speculated that the pET14 plasmid failed to show proper overexpress because of an issue with the T7 promoter or stop codon however, this was never confirmed. Using the restriction sites Xba1 and Xho1 the LipN sequence was removed from the pET14 plasmid and cloned into the pET28a plasmid.

The LipN DNA encoded in pET28 plasmid was transformed into DH5α *E. coli* cells using the antibiotics Kanamycin and chloramphenicol as selective markers. The plasmid was then isolated and purified from *E. coli* cell contents using alkaline lysis in conjunction with DNA affinity columns. The DNA concentration of the purified plasmid was then analyzed and pooled together and diluted to approximately 70 ng/μL using deionized water (Table 1A and B). The molecular cloning of the LipN sequence into the pET28a plasmid vector was confirmed via sequencing. T7 forward and T7 reverse primers were used and the sequencing results were evaluated using Expasy translate and BLAST (*Figure 6*). The sequence showed a 100% match to lipase from *Mycobacterium,* confirming the LipN sequence. The experimental LipN sequence showed a 100% match to the theoretical LipN amino acid sequence from the pET14

plasmid purchased from The Seattle Structural Genomics Center for Infectious Disease[13] (*Figure 6*).

Table 1A: Average DNA concentrations of LipN plasmid.

Sample	DNA concentration (ng/µL)
1	175.4
2	179.9
3	110.1
4	73.7

Table 1B: Average DNA concentrations of pooled and diluted LipN plasmid samples.

Sample	DNA concentration (ng/µL)
1	75
2	73

FCLTLRRRYTMAHHHHHHMGTLEAQTQGPGSMTNSLPGETDLHPETVHATMS
WLSRVQNTVTVVGAKVIPWVPDVAKRLITRGRSVIIDGNTLDPALQLMLSGMR
VVGLDGLVIDDDLAASRAHMREAMLGFPGPQIHVDVEELTLPGPAGDISARHY
RPPGDAAAPLLVFYHGGGWALGDLDTHDAVCRLTCRDAGIHVLAIDYRLSPEH
RAPAAIDDAFAAFEWAHAHAAELGALPGRVAVGGDSAGGNLAAVVSQLARDS
GGPAPIFQWLIYPRTDFAGRTRSASLFARGFLLTKRDIDWFHSQYLKGSGIEPTD
PRVSPLRAESLAGLAPALIAVAGFDPLRDEGENYATALRAAGTPVDLRAMGSL
THGFLNLFPLGGGCAAATSELISALRAHLTRV--TARTSSAAKLLEHHHHHH-
DPAANKA

Figure 6: Expasy translate results of the overlap of the T7 forward and T7 reverse primer of the LipN pET28a plasmid. The LipN amino acid sequence is shown in red.

Purification and IPTG Induced Overexpression

The cloned *M. ulcerans* LipN protein was overexpressed in *E. coli* host (strain BL21-DE3) grown under selective pressure using chloramphenicol and kanamycin antibiotic, and induced with isopropylthiogalactiside (IPTG). The LipN protein was purified from other *E. coli* soluble components via Ni-NTA affinity chromatography and eluted with increasing concentration of imidazole followed by dialysis against phosphate-buffered saline solution. The identity and purity of the LipN protein was

confirmed by sodium Dodecyl Sulfate-PolyAcrylamide Gel Electrophoresis (SDS-PAGE).

SDS-PAGE is used to confirm the presence of a protein based on the expected molecular weight and allows for detection of any protein contaminants left over from the *E. coli* host cells. The expected molecular weight for the cloned LipN protein is 41.7 kD based on the amino acid sequence. The SDS-PAGE gel showed a large band around 40 kD, which corresponds to the expected molecular weight of the LipN protein, confirming the successful overexpression and identity of the LipN protein. The only other visible band appears around 14kDa, which is the molecular weight of lysozyme. This impurity was most likely left over from the lysis of the cultured *E. coli* cells.

Overall, the SDS-PAGE gel confirmed the presence of a relatively pure solution of LipN protein (Figure 7).

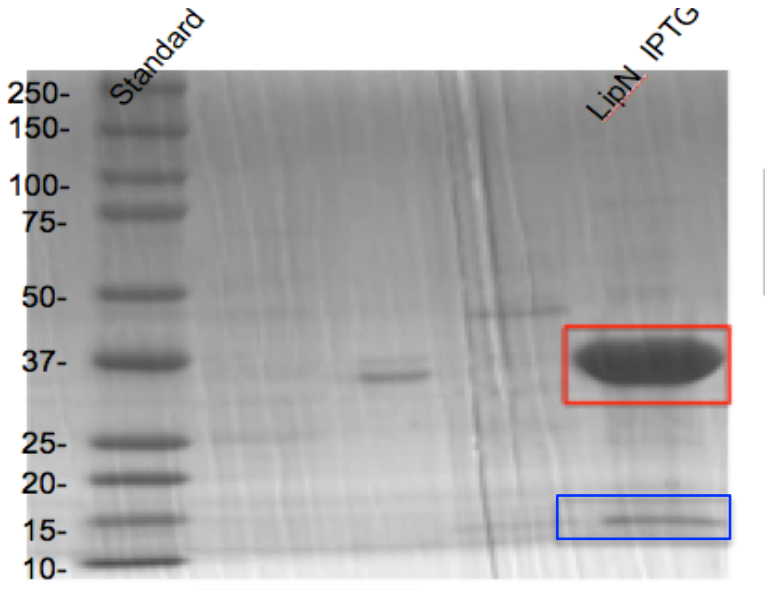

Figure 7: SDS-PAGE of LipN induced with IPTG. The two important lanes are labeled; the standard marker with the corresponding molecular weight values and the LipN protein sample. The overexpressed LipN band appears around 40kDa corresponding to the predicted molecular weight of 41.7kDa for the cloned LipN protein. The only other band, 14kDa, is predicted to be lysozyme.

Protein Concentration

The concentration of LipN in solution was quantitated by ultraviolet light absorption spectroscopy, using the theoretical extinction coefficient for LipN of $\Sigma_{280} = 4.2x10^4\ M^{-1}cm^{-1}$. The purified LipN protein has an average concentration of 2.25 mg/mL (Table 2).

Table 2: Protein Concentration of LipN quantitated by ultraviolet light absorption spectroscopy.

Sample	Protein Concentration (mg/mL)
1	2.07
2	2.43
Average	2.25

Thermal Stability

The thermal stability of LipN was measured by differential scanning fluorimetry using SYPRO orange dye[25]. The midpoint of the thermal denaturation curve (T_m value) was measured in triplicate and each value yielded a melting temperature of 43°C (Figure 8). Based on the thermal stability it can be predicted that the LipN protein will not denature during the kinetic assays that were ran at 24°C.

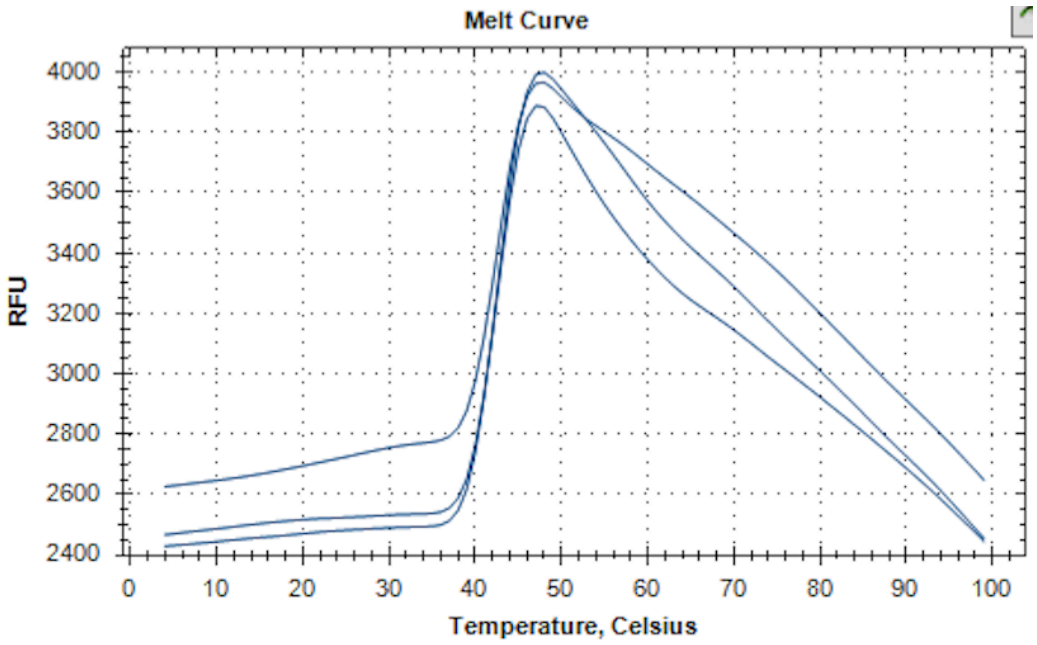

Figure 8: Thermal Stability assay of LipN using differential scanning fluorimetry. The relative fluorescent units (RFU) are plotted against temperature. The unfolding of the LipN protein and exposure of buried hydrophobic areas leads to increased binding of SYPRO Orange dye. The T_m value is the midpoint of the protein unfolding transition and was calculated in triplicate as depicted by the three separate melting curves[25]. The T_m value for LipN was calculated to be 43.0°C.

Substrate Specificity of LipN

An approach to gaining a comprehensive understanding of enzymes such as LipN is through analyzing the enzyme's substrate specificity and binding affinity through a highly accurate enzymatic assay. The substrate specificity of LipN was elucidated by the relative rate of hydrolysis of the library of Fluorogenic esters catalyzed by LipN. The hydrolysis reaction converts a non-fluorescent ester substrate into a fluorescent product, fluorescein. The reaction is negligibly slow in absence of a catalyst and the rate of appearance of fluorescence is dependent on the efficacy of catalysis with a given substrate.

The overall efficiency at which LipN catalyzed the hydrolysis reaction for the latent fluorogenic ester substrates (*Figure 5*) was quantitated as the k_{cat}/K_M ratio. The

LipN enzyme showed the highest enzymatic activity for substrate number 6, di(methoxyacetoxymethyl ether), yielding a k_{cat}/K_M ratio of 881 $M^{-1}s^{-1}$. The high overall enzymatic activity of LipN with substrate 6 is based more on the efficiency of the enzyme than the binding interactions. LipN catalyzed substrate 6 with the greatest efficiency ($k_{cat} = 3.6 \times 10^{-3}$ s^{-1}) but relatively weak binding interactions ($K_M = 4.1$ M) compared to the other fluorogenic ester substrates (*Table 3*).

The enzyme showed some activity on the alkyl ester substrates 2 (k_{cat}/K_M = 140 $M^{-1}s^{-1}$), 3 (k_{cat}/K_M = 89 $M^{-1}s^{-1}$), and 4 (k_{cat}/K_M ratio = 87$M^{-1}s^{-1}$), implying that LipN prefers two to four carbon chain alkyl ester substrates. The bulky cycloalkyl esters, tertiary ester, unsaturated ester, and fluorinated esters were poor substrates based on their low enzymatic activity with the exception of the fluorinated ester substrate 15 and the cycloalkyl ester substrate 9.

Substrate 9, di(cyclobutanecarboxymethyl ether), and substrate 15, di(trifluoropropionoxymethyl ether), where the exceptions to the general tend and yielded a k_{cat}/K_M ratio of 48 $M^{-1}s^{-1}$and 80 $M^{-1}s^{-1}$ respectively. Substrate 9 is the least bulky compared to the other cycloalkyl ester substrates and the unsaturated and tertiary ester, implying that the enzyme is inefficient at hydrolyzing substrates having larger, bulky acyl R groups but is able to hydrolyze smaller cycolalkyl ester substrates. The binding interactions of substrate 9 and substrate 6 were similar, $K_M = 4.2$ M and $K_M =$ 4.1 M respectively, but the catalytic efficiency of LipN was lower for substrate 9, $k_{cat} = 2.0 \times 10^{-4}$ s^{-1}. Aside from preferring short chain, non-bulky ester derivatives, the LipN enzyme seems to have greater catalytic efficiency with substrates containing a

heteroatom. This assumption was further verified by analysis of the overall catalytic efficiency of LipN with the fluorinated ester substrates.

LipN showed minuscule enzymatic activity for the bulky fluorinated ester substrates 13 and 14; however, LipN catalyzed the non-bulky fluorinated ester substrate 15 with overall efficiency close to that of the alkyl ester substrates 3 and 4. Substrate 15 yielded a k_{cat}/K_M of 80 $M^{-1}s^{-1}$, substrate 3 yielded a k_{cat}/K_M of 89 $M^{-1}s^{-1}$, and substrate 4 yielded a k_{cat}/K_M of 87 $M^{-1}s^{-1}$(*Table 3*). Although the overall catalytic efficiency of LipN for substrates 2, 3, and 15 is similar there are deviations between the k_{cat} and K_M values.

The alkyl ester substrates gave small k_{cat} and K_M values suggesting that LipN catalyzes the substrates with low efficiency but forms strong binding interactions. Listed in numerical order starting with substrate 2: k_{cat} 1.3×10^{-4} s^{-1}, K_M = 0.9 M; k_{cat} 3.3×10^{-5} s^{-1}, K_M = 0.37 M; k_{cat} 5.8×10^{-5} s^{-1}, K_M = 0.7 M. Conversely, LipN showed to form weak binding interactions (K_M = 30 M) with the fluorinated ester substrate 15 but higher catalytic efficiency ($k_{cat} = 2.4 \times 10^{-3}$ s^{-1}) compared to the alkyl ester substrates 2 and 3. Comparing substrate 15 (a two carbon fluorinated ester) to substrate 2 (a two carbon alky ester) we can deduce the relative effect of the fluorine on the catalytic activity of LipN. The fluorine atom decreased the binding interaction, as seen by a larger K_M value, but increased the catalytic efficiency (k_{cat}) of the enzyme (*Table 3*).

Overall, LipN prefers non-bulky 2-4 carbon chain substrates. The highest overall catalytic efficiency was seen for the alkyl ether ester substrate 6. LipN showed some enzymatic activity for the alkyl ester substrates 2, 3, and 4, which formed strong

binding interactions but yielded low catalytic efficiency. The enzymatic activity seen with substrate 9 and substrate 15 indicate that the enzyme is more efficient at catalyzing the hydrolysis of a short carbon chain ester substrate that contains a heteroatom.

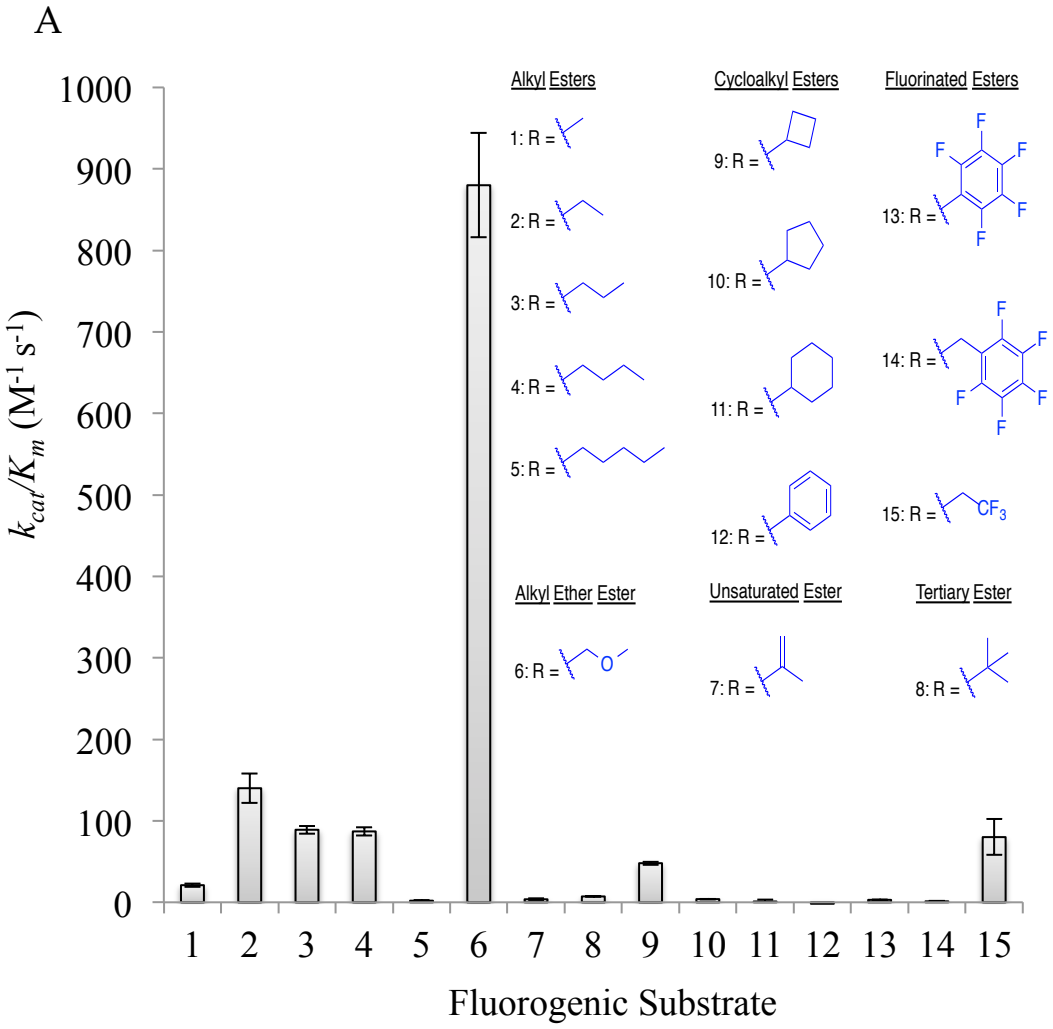

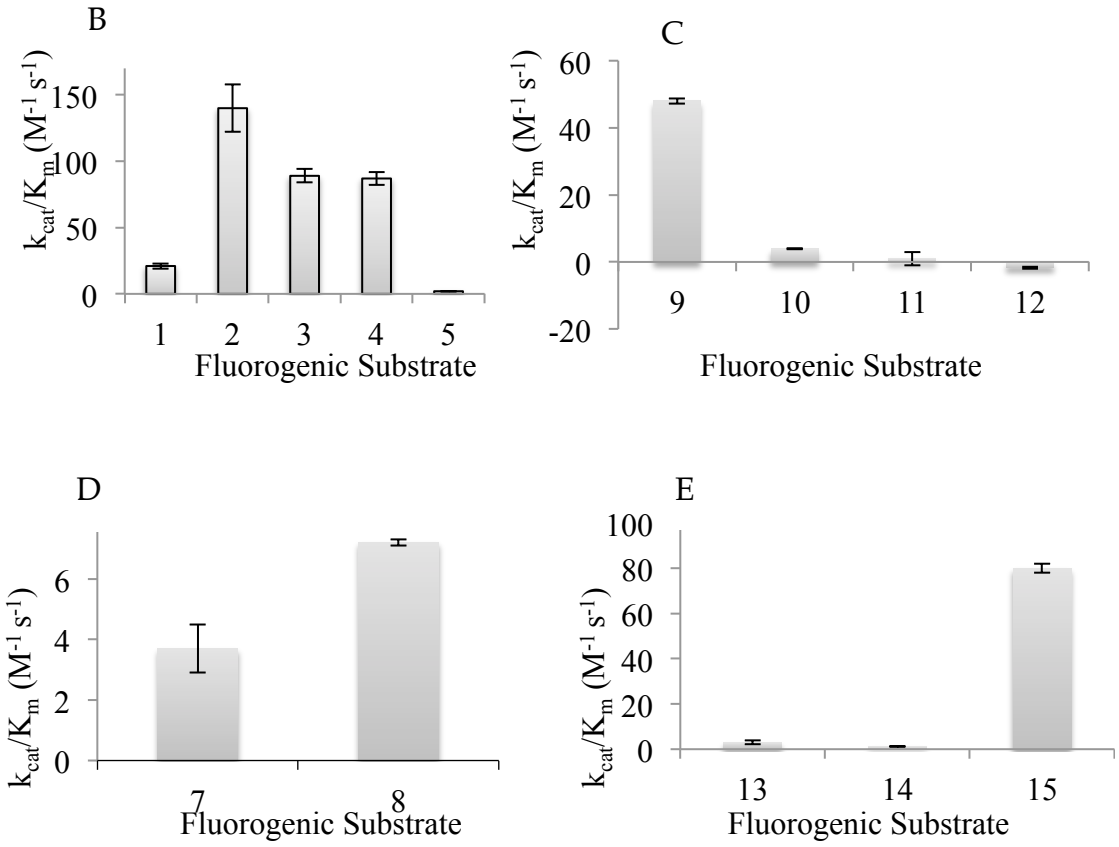

Figure 9: (A) Overall catalytic efficiency (k_{cat}/K_M) of LipN with each of the 15 latent fluorogenic substrates with the chemical identity of the acyl R-groups. To show patterns within the different classes of substrates, important subclasses are compared: (B) alkyl esters (C) cycloalkyl esters (D) unsaturated ester and tertiary ester (E) fluorinated esters.

Table 3: Michaelis-Menten constants*:* K_M, k_{cat}, k_{cat}/K_M for the library of 15 Latent fluorogenic ester substrates with error analysis.

Substrate	k_{cat} (s^{-1})	K_M (M)	k_{cat}/K_M ($M^{-1}s^{-1}$)
1	$1.2 \times 10^{-5} \pm 7 \times 10^{-7}$	0.58 ± 0.14	21 ± 2
2	$1.3 \times 10^{-4} \pm 7 \times 10^{-6}$	0.9 ± 0.24	140 ± 18
3	$3.3 \times 10^{-5} \pm 9 \times 10^{-7}$	0.37 ± 0.06	89 ± 5
4	$5.8 \times 10^{-5} \pm 3 \times 10^{-6}$	0.7 ± 0.2	87 ± 5
5	$7.7 \times 10^{-6} \pm 3 \times 10^{-7}$	3.8 ± 0.7	2 ± 0.2
6	$3.6 \times 10^{-3} \pm 2 \times 10^{-4}$	4.1 ± 0.6	881 ± 64
7	$2.1 \times 10^{-5} \pm 1 \times 10^{-6}$	7 ± 3	3.7 ± 0.8
8	$7.9 \times 10^{-5} \pm 1 \times 10^{-6}$	10.6 ± 0.5	7.2 ± 0.1
9	$2.0 \times 10^{-4} \pm 5 \times 10^{-6}$	4.2 ± 0.5	48 ± 2
10	$1.1 \times 10^{-4} \pm 7 \times 10^{-6}$	29 ± 4.6	3.9 ± 0.3
11	$1.3 \times 10^{-5} \pm 2 \times 10^{-6}$	11.9 ± 5.4	1 ± 2
12	$2 \times 10^{-7} \pm 8 \times 10^{-8}$	-0.12 ± 0.02	-1 ± 0.7
13	$4.2 \times 10^{-4} \pm 2 \times 10^{-5}$	0.125 ± 0.005	3 ± 0.1
14	$2.3 \times 10^{-4} \pm 4 \times 10^{-5}$	188 ± 49	1.2 ± 0.3
15	$2.4 \times 10^{-3} \pm 3 \times 10^{-4}$	30 ± 11	80 ± 22

Conclusion

Mycobacterium ulcerans is the causative agent of the ulcerative skin disease Buruli ulcer, which currently has limited treatment options available. Lipolytic enzymes have been shown to be potential drug targets based on their prevalence in mycobacteria and importance in mediating necessary cellular functions. LipN is one proposed serine hydrolase of *M. ulcerans* that has gained recent attention in the scientific literature. The natural physiological substrate and biological role of the LipN protein has not been revealed. Therefore, studies focused on analyzing the structure-function relationship of the LipN enzyme provide data of basic biochemical interest. Throughout Butler Summer Institute and my senior year at Butler University, I investigated the substrate specificity of the LipN enzyme by measuring its enzymatic activity against a library of 15 latent fluorophore ester substrates. Steady state enzymatic kinetic data was fit to the Michaelis-Menten equation; k_{cat}, K_M, k_{cat}/K_M constants were derived to quantitate the

structure-activity relationships that will provide insight into the substrate specificity of LipN.

The LipN protein showed preference for non-bulky 2-4 carbon chains with the greatest enzymatic activity for an alky ether ester substrate with a k_{cat}/K_M of 881±64 $M^{-1}s^{-1}$. The affect of heteroatoms on the overall catalytic activity of the LipN enzyme is not fully understood. Heteroatoms may increase the catalytic efficiency of the enzyme but reduce the binding interactions between the enzyme and the substrate. This pattern was seen for substrate 6 and substrate 15, both of which are short chain carbon substrates with a heteroatom. These two substrates showed the greatest catalytic efficiency out of all the substrates tested, yielding a $k_{cat} = 3.6 \times 10^{-3}$ s^{-1} and $k_{cat} = 2.4\times 10^{-3}$ s^{-1}, respectively. However, the binding interactions of substrate 6 ($K_M = 4.2$ M) and substrate 15 ($K_M = 30$ M) were weak. Expansion of the substrate library to include short carbon chains containing heteroatoms is needed to gain a full understanding of the effect heteroatoms have on the enzymatic activity of LipN.

Future studies will be directed at gaining a more holistic understanding of the substrate specificity of the LipN enzyme by using additional latent fluorophore substrates: specifically, substrates with short carbon chains containing heteroatoms. Site-directed mutagenesis of the proposed active site residues would also help to reveal the structure-function relationship of the LipN protein. Furthermore, crystalizing the LipN protein will provide a more global understanding of the structure of LipN and will allow for more detailed structural comparisons between the LipN protein of *M. ulcerans* and the LipN protein of other mycobacteria.

References

1. Buruli ulcer WHO Annual Meeting on Buruli ulcer. 2011. World Health Organization. Retrieved from: http://www.who.int/buruli/information/Buruli_meeting_Abstracts_2011_ENG.pdf?ua=1.
2. Douglas S. Walsh, Francoise Portaels, Wayne M.Meyers. 2008. Buruli ulcer (*Mycobacterium ulcerans* infection). *The Royal Society of Tropical Medicine and Hygiene* 102: 969-978.
3. Douglas S. Walsh, Francoise Portaels, Wayne M.Meyers. 2011. Buruli Ulcer: Advances in Understanding *Mycobacterium ulcerans* Infection. *Dermatologic Clinics*. 29(1): 1-8.
4. Laurent Marsollier, Nadine Honoré, Pierre Legras, Anne LIse Manceau, Henri Kouakou, Bernard Carbonnelle, and Stewart T. cole. 2003. Isolation of Three *Mycobacterium ulcerans* Strains Resistant to Rifampin after Experimental Chemotherapy of Mice. *Anitmicrob. Agents Chemother*. 47(4): 1228-1232.
5. Marcus Beissner et al. 2010. A Genotypic Approach for Detection, Identification, and Characterization of Drug Resistance in *Mycobacterium ulcerans* in Clinical Samples and Isolates from Ghana. *Am J Trop Med Hyg*. 83(5): 1059-1065.
6. L. Dedieu, C. Serveau-Auesque, L. Kremer, S. Canaan. 2012. Mycobacterial lipolytic enzymes: A gold mine for tuberculosis research. *Biochimie*. 95: 66-73
7. Daniel A. Bachovchin and Benjamin F. Cravatt. 2013. The Pharmacological Landscape and Therapeutic Potential of Serine Hydrolases. *Nat Rev Drug Discov*.; 11(1): 52-68.
8. Gurdyal Singh, Gurpreet Singh, Dipendrasinh Jadeja, and Jagdeep Kaur. 2012. Lipid hydrolyzing enzymes in virulence: Mycobacterium tuberculosis as model system. *Critical Review in Microbiology*. 36(3): 259-269.
9. David, N.L, Cox, M.M. 2008. *Lehninger Principles of Biochemistry*. Fifth Edition W. H Freeman and Company: New York.
10. Grazia M. Borrelli et al. 2015. *Int. J. Mol. Sci.*
11. Timothy P. Stinear et al. 2007. Reductive evolution and niche adaptation inferred form the genome of *Mycobacterium ulcerans*, the causative agent of Buruli ulcer. *Genome Res* 17: 192-200.
12. Dipendrasinh Jadeja, Nandita Dogra, Stuti Arya, Gurpreet Singh, Gurdyal Singh, Jagdeeo Kaur. 2015. Characterization of LipN(Rv2970c) of *Mycobacterium tuberculosi*s H37Rv and its probable role in xenobiotic degradation. *Journal of Cellular Biochemistry*: 10.1002/jcb.25285.
13. Loren Baugh et al. 2015. Increasing the structural coverage of tuberculosis drug targets. *Tuberculosis*. 95:142-148.
14. P.J Myler et al. 2009. The Seattle Structural Genomics Center for Infectious Disease (SSGCID). *Infect Disord Drug Targets*. 9(5): 493-506
15. Luke D. Lavis and Ronald T. Raines. 2008. Bright Ideas for Chemical Biology. *American Chemical Society*. 10.1021/cb700248m.
16. Luke D. Lavis, Tzu-Yuan Chao, and Ronald T. Raines. 2010. Synthesis and utility of Fluorogenic acetoxymethyl ethers. *The Royal Society of Chemistry*.

DOI: 10.1039/c0sc00466a.
17. Lin Tian et al. 2011. Selective esterase-ester pair for targeting small molecules with cellular specificity. *PNAS Early Edition*. doi: 10.1073/pnas.1111943109.
18. Elizabeth E. Ellis, Chinessa T. Adkins, Natalie M. Galovska, Luke D. Lavis, and R. Jeremy Johnson. 2013. Decoupled Roles for the Atypical, Bifurcated Binding Pocket of the ybfF Hydrolase. *ChemBioChem.* 14: 1134-1144.
19. Jessica K. Lukowski, Christopher P. Savas, Alexandra M. Gehring, Magy G. McKary, Chinessa T. Adkins, Luke D. Lavis, Geoffrey C. Hoops, and R. Jeremy Johnson. 2014. Distinct Substrate Selectivity of a Metabolic Hydrolase from *Mycobacterium tuberculosis*. *Biochemistry.* 53: 7386-7395.
20. Matthew K. Hedge. Alexandra M. Gehring. Chinessa T. Adkins, Leigh A Weston, Luke D. Lavis, R. Jeremy Johnson. 2012. The structural basis for the narrow substrate specificity of an acetyl esterase from Thermotoga maritime. Elsevier doi: 10.1016/j.bbapap.2012.05.009
21. Novagen. 2002. pET System Manual (10^{th} edition).
22. IBI Scientific. High-Speed Plasmid Mini Kit.
23. Shane A. Seabrook and Janet Newman. 2013. High-Throughput Thermal Scanning for Protein Stability: Making a Good Technique More Robust. *American Chemical Society*. 15: 387-392.
24. Anton Simeonov. 2013. Recent developments in the use of differential scanning fluorometry in protein and small molecule discovery and characterization. *Expert Opin. Drug Discov*. 8(9): 1071-1082.
25. R. Jeremy Johnson, Christopher J. Savas, Zachary Kartje, and Geoffrey C. Hoops. 2014. Rapid and Adaptable Measurement of Protein Thermal Stability by Differential Scanning Fluorimetry: Updating a Common Biochemical Laboratory Experiment. *American Chemical Society. 92:1077-1080*

Appendix A
Fluorescein di(acetoxymethyl ether) ACME
Substrate #1

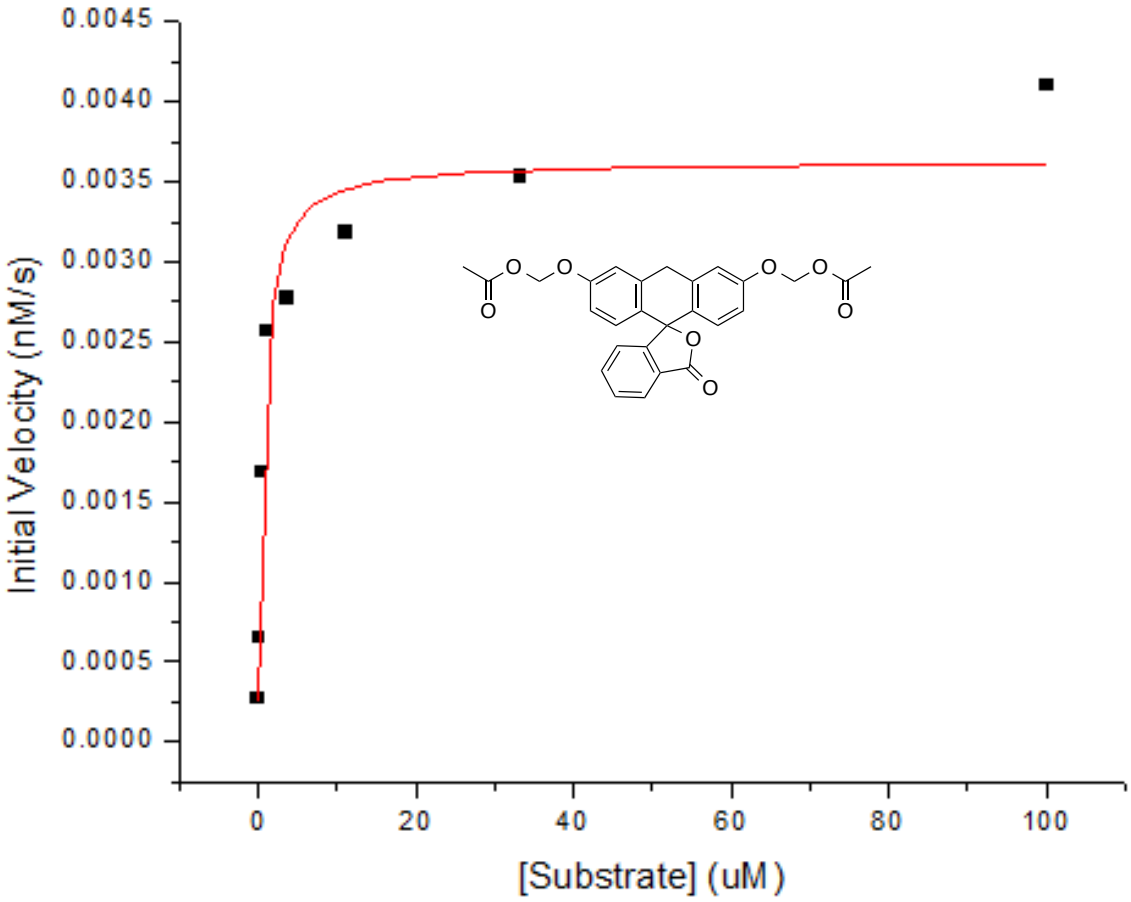

Chi^2/DoF	8.2483E-8	
R^2	0.96207	
V_{MAX}	0.004	±0.0002
K_M (M)	0.58	±0.14
K_{cat} (s^{-1})	0.000012	±4.7E-07

Fluorescein di(propionoxymethyl ether) PRME
Substrate #2

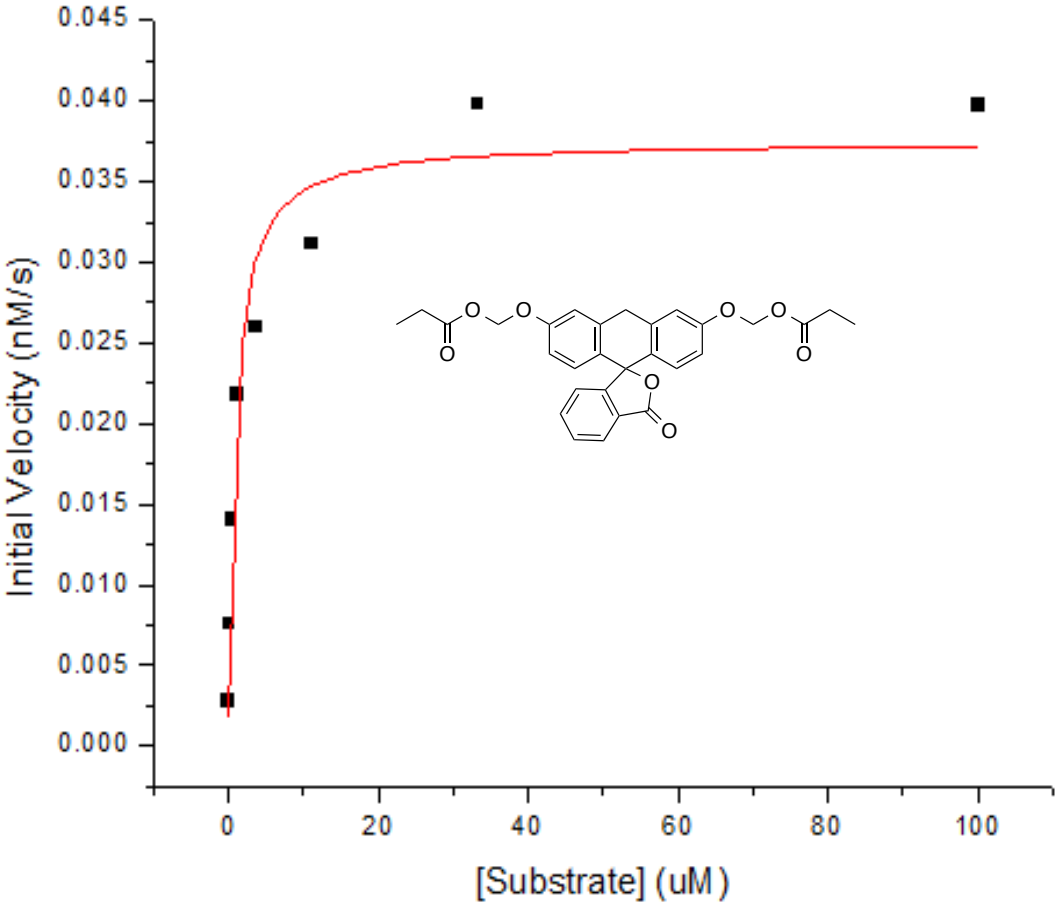

Chi^2/DoF	0.00001	
R^2	0.95583	
V_{MAX}	0.038	±0.002
K_M (M)	0.9	±0.24
K_{cat} (s^{-1})	0.000125	±7E-06

Fluorescein di(butyloxymethyl ether) BUME
Substrate #3

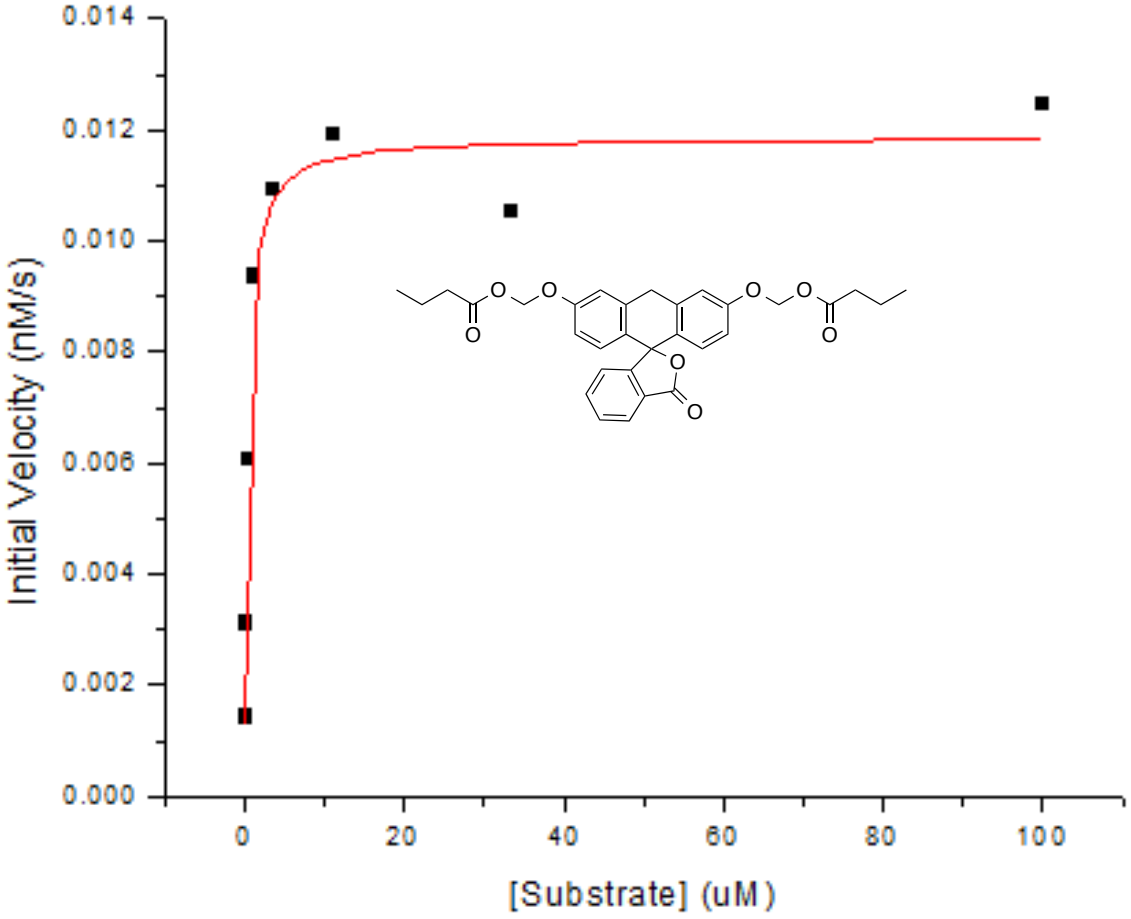

Chi^2/DoF	3.7464E-7	
R^2	0.98163	
V_{MAX}	0.0119	±0.00034
K_M (M)	0.37	±0.06
K_{cat} (s^{-1})	3.3E-5	±9E-7

Fluorescein di(valeryloxymethyl ether) VLME
Substrate #4

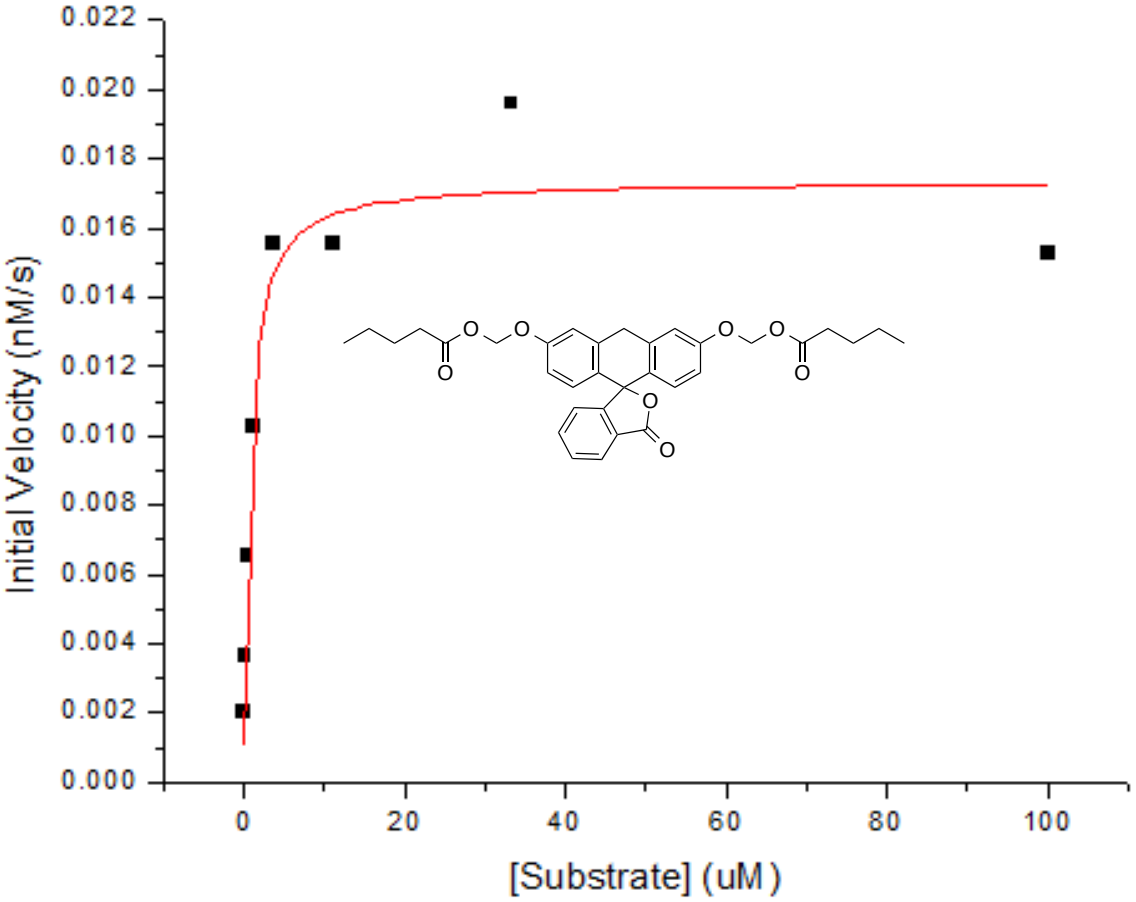

Chi^2/DoF	2.3786E-6	
R^2	0.95067	
V_{MAX}	0.0174	±0.0009
K_M (M)	0.7	±0.2
K_{cat} (s^{-1})	5.8.3E-5	±3E-6

Fluorescein di(hexanoylxymethyl ether) HXME
Substrate #5

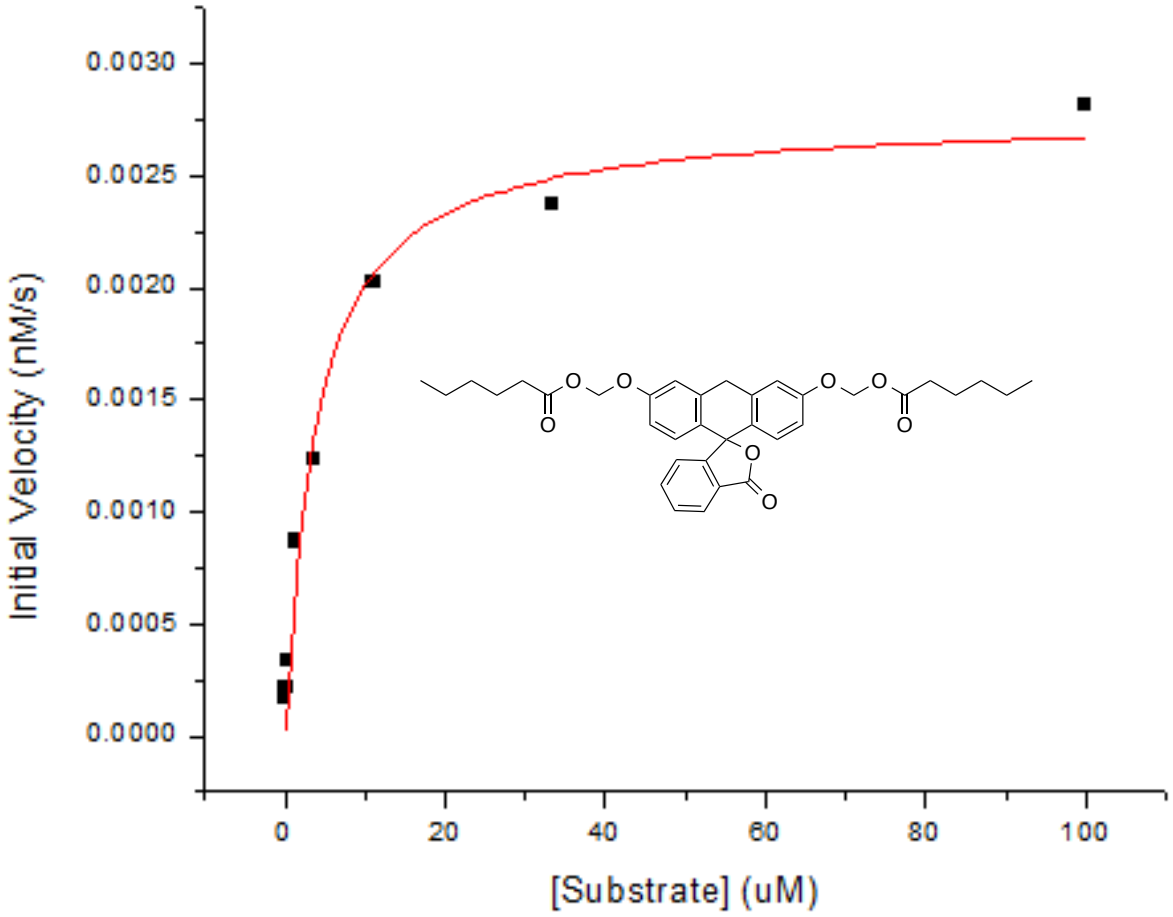

Chi^2/DoF	2.081E-8	
R^2	0.98343	
V_{MAX}	0.0028	±0.0001
K_M (M)	3.8	±0.7
K_{cat} (s^{-1})	7.7E-6	±3E-7

Fluorescein di(methoxyacetoxymethyl ether) MOAME
Substrate #6

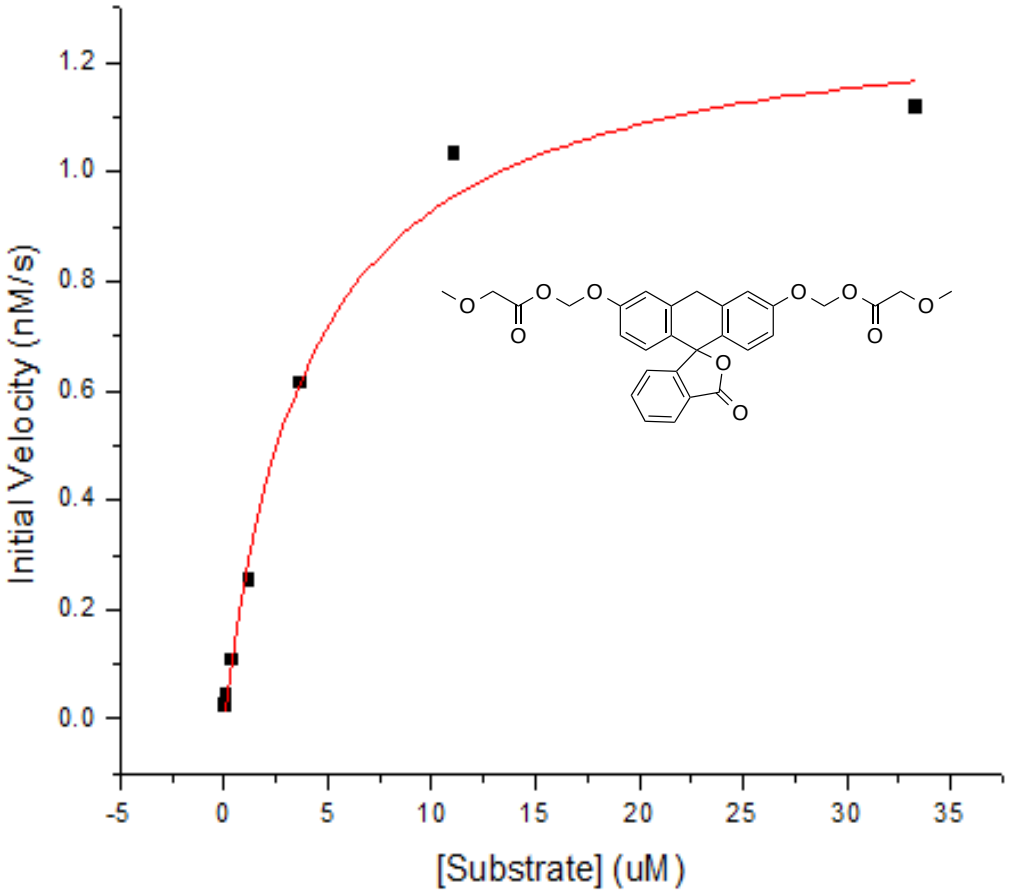

Chi^2/DoF	0.00217	
R^2	0.99176	
V_{MAX}	1.31	±0.06
K_M (M)	4.1	±0.6
K_{cat} (s^{-1})	3.6E-3	±2E-4

Fluorescein di(methacryloxymethyl ether)
Substrate #7

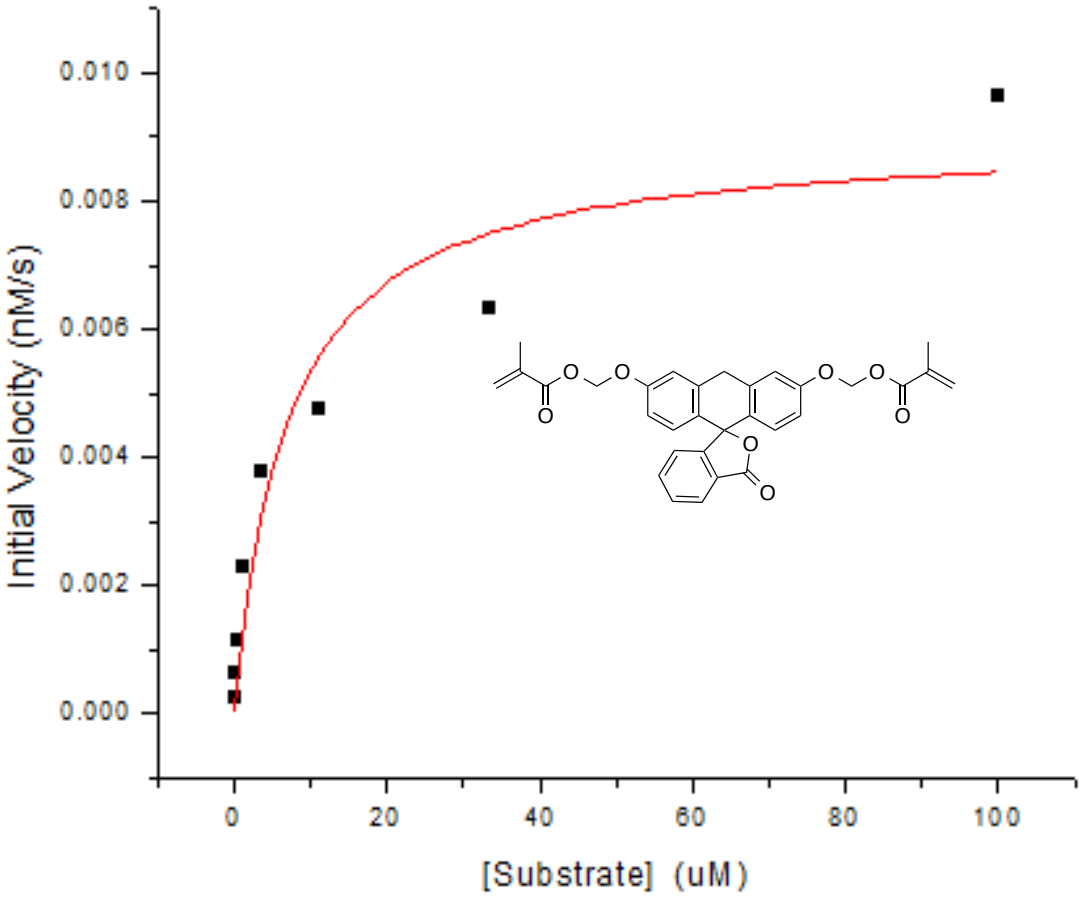

Chi^2/DoF	8.8076E-7	
R^2	0.92783	
V_{MAX}	0.009	±0.00098
K_M (M)	7	±3
K_{cat} (s^{-1})	2.1E-5	±1E-6

Fluorescein di(pivyloxymethyl ether) PVME
Substrate #8

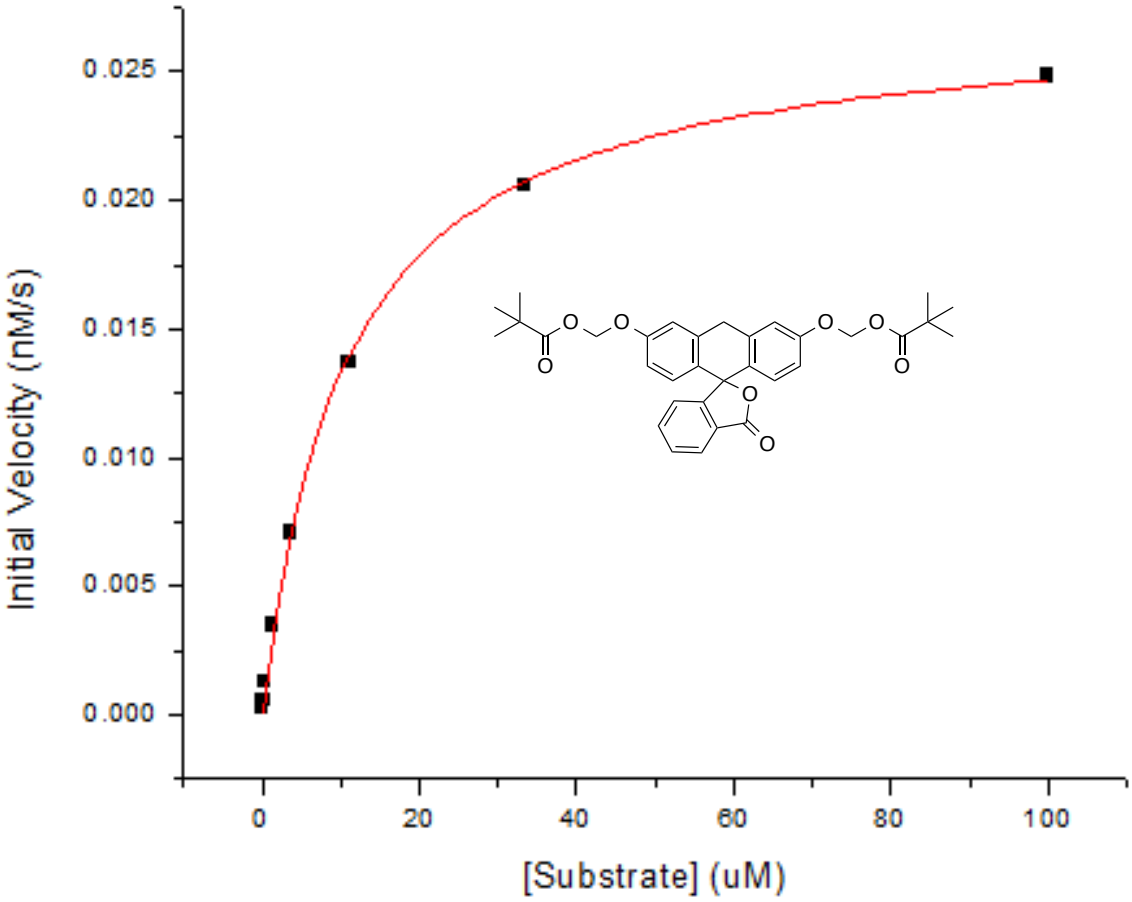

Chi^2/DoF	1.0878E-7	
R^2	0.999	
V_{MAX}	0.0273	±0.0004
K_M (M)	10.6	±0.5
K_{cat} (s^{-1})	7.9E-5	±1E-6

Fluorescein di(cyclobutanecarboxymethyl ether) CBME
Substrate #9

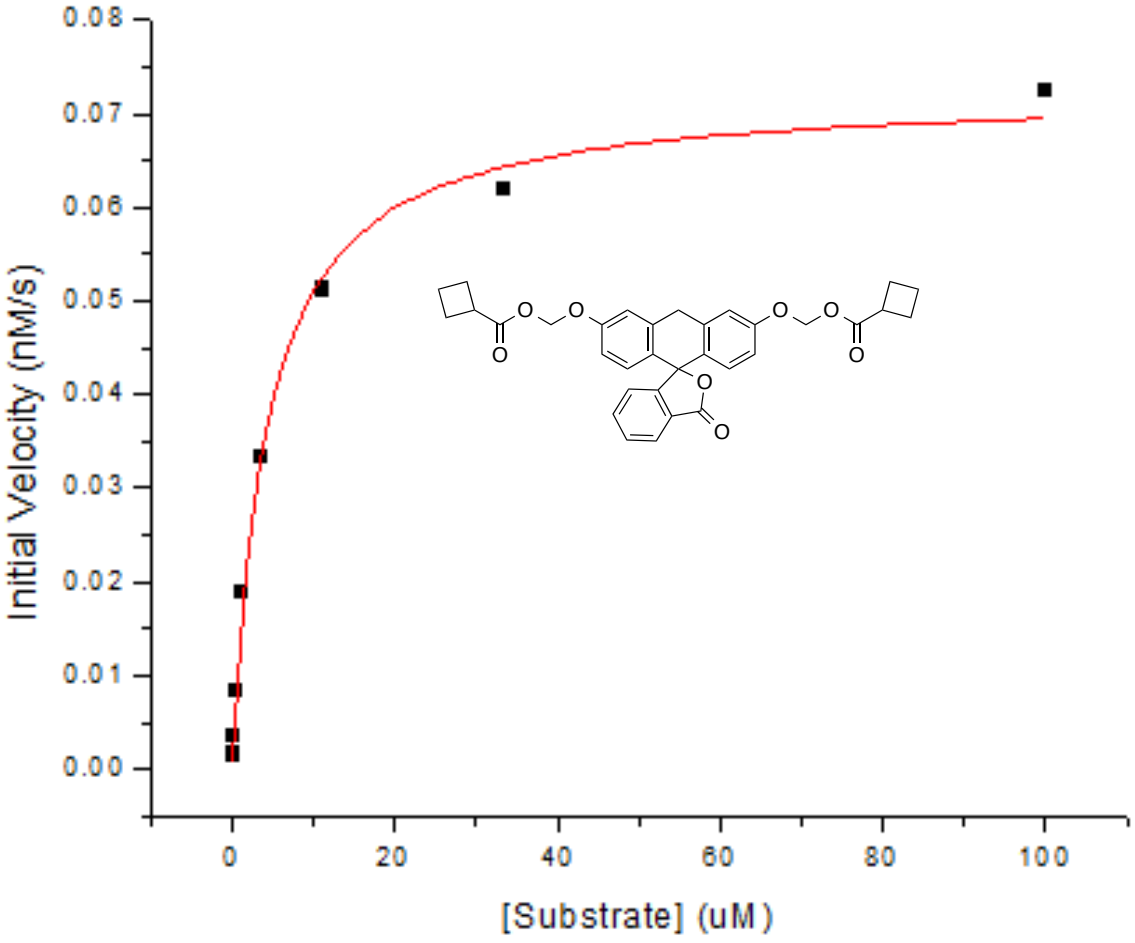

Chi^2/DoF	4.8073E-6	
R^2	0.99463	
V_{MAX}	0.072	±0.002
K_M (M)	4.2	±0.5
K_{cat} (s^{-1})	0.00020	±5E-6

Fluorescein di(cyclopentanecarboxymethyl ether) CPME
Substrate #10

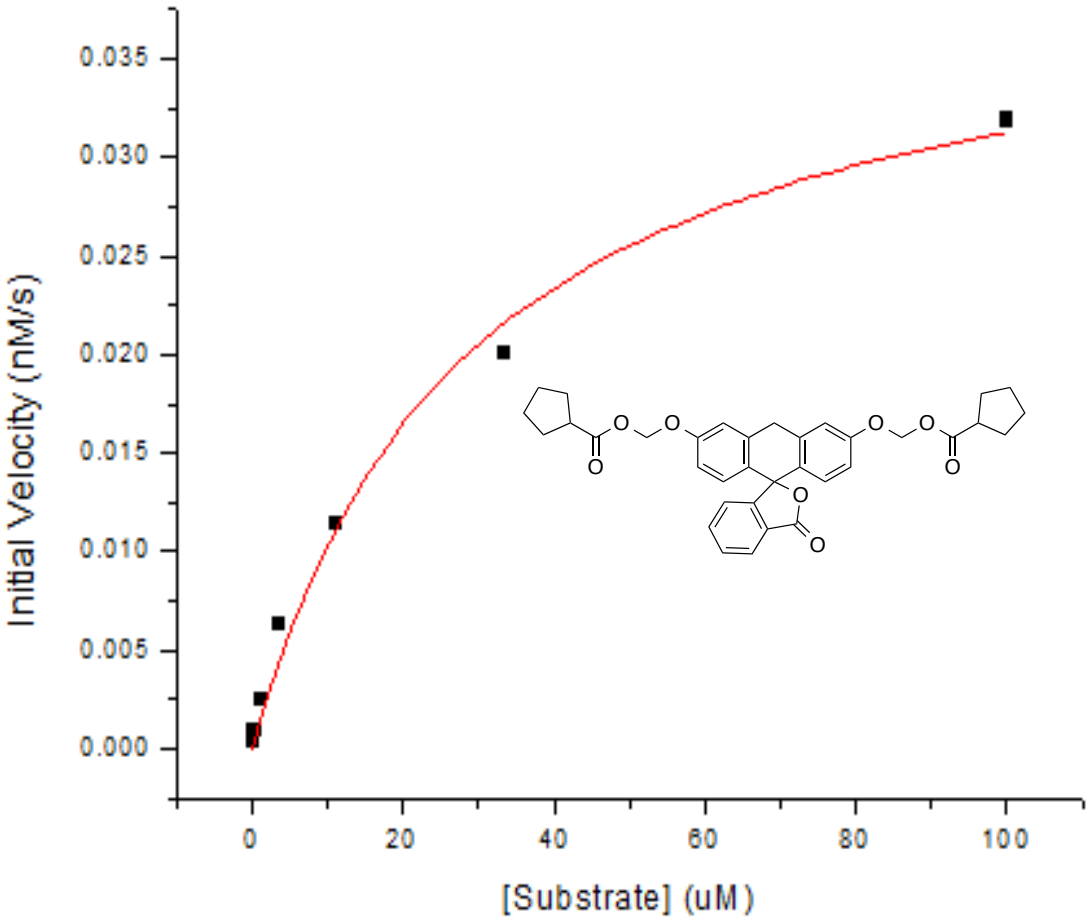

Chi^2/DoF	1.1831E-6	
R^2	0.99218	
V_{MAX}	0.040	±0.002
K_M (M)	29	±4.6
K_{cat} (s^{-1})	0.00011	±7E-6

Fluorescein di(cyclohexanecarboxymethyl ether) CHME
Substrate #11

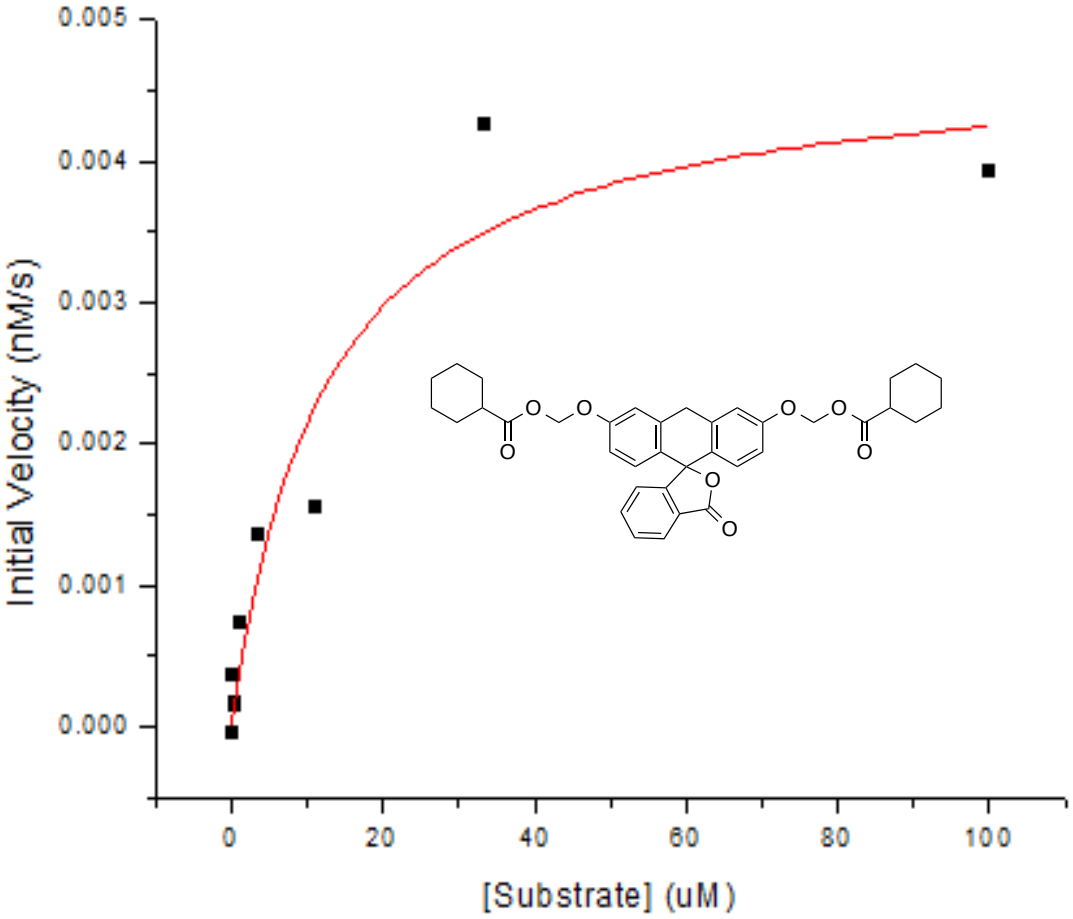

Chi^2/DoF	2.4268E-7	
R^2	0.92584	
V_{MAX}	0.0048	±0.0007
K_M (M)	11.9	±5.4
K_{cat} (s^{-1})	1.3E-5	±2E-6

Fluorescein di(benzoyloxymethyl ether) BNME
Substrate #12

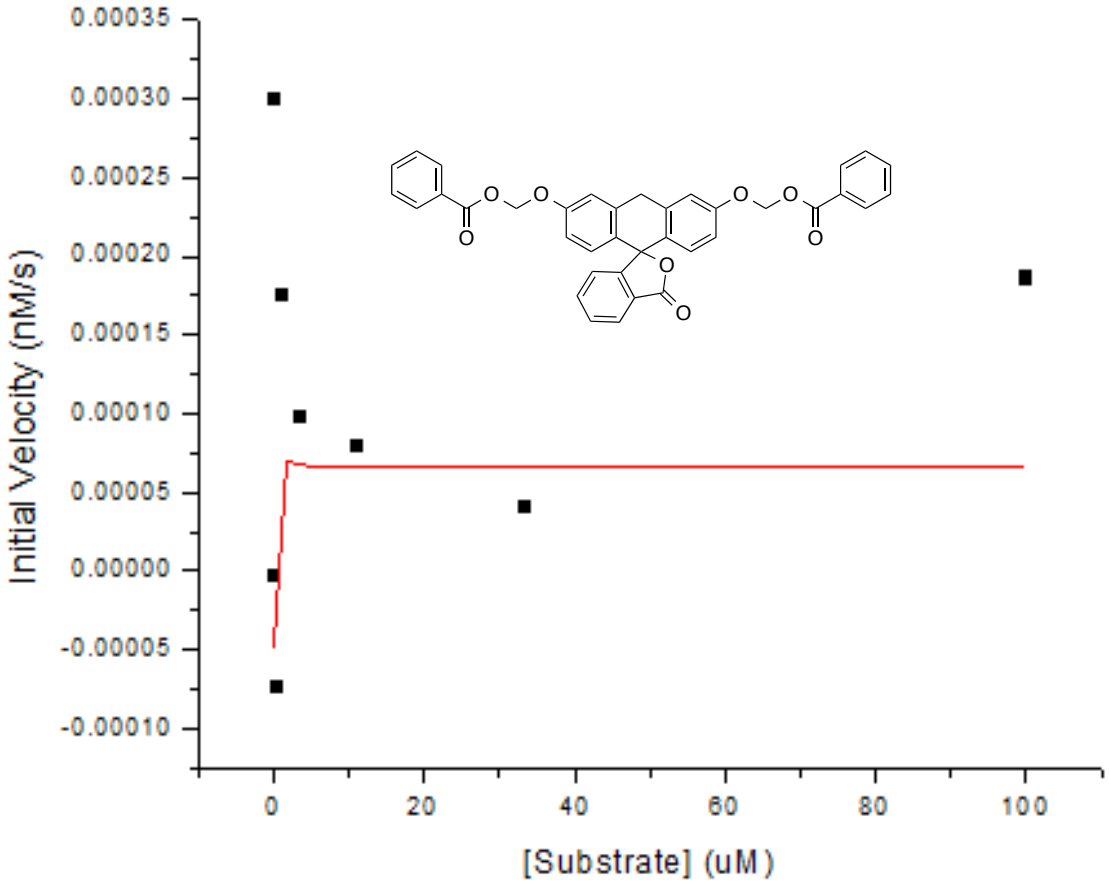

Chi²/DoF	9.2497E-9	
R^2	0.43231	
V_{MAX}	0.00007	±0.00003
K_M (M)	-0.12	±0.02
K_{cat} (s^{-1})	2E-7	±8E-8

Fluorescein di(pentafluorobenzoyloxymethyl ether) FBME
Substrate 13

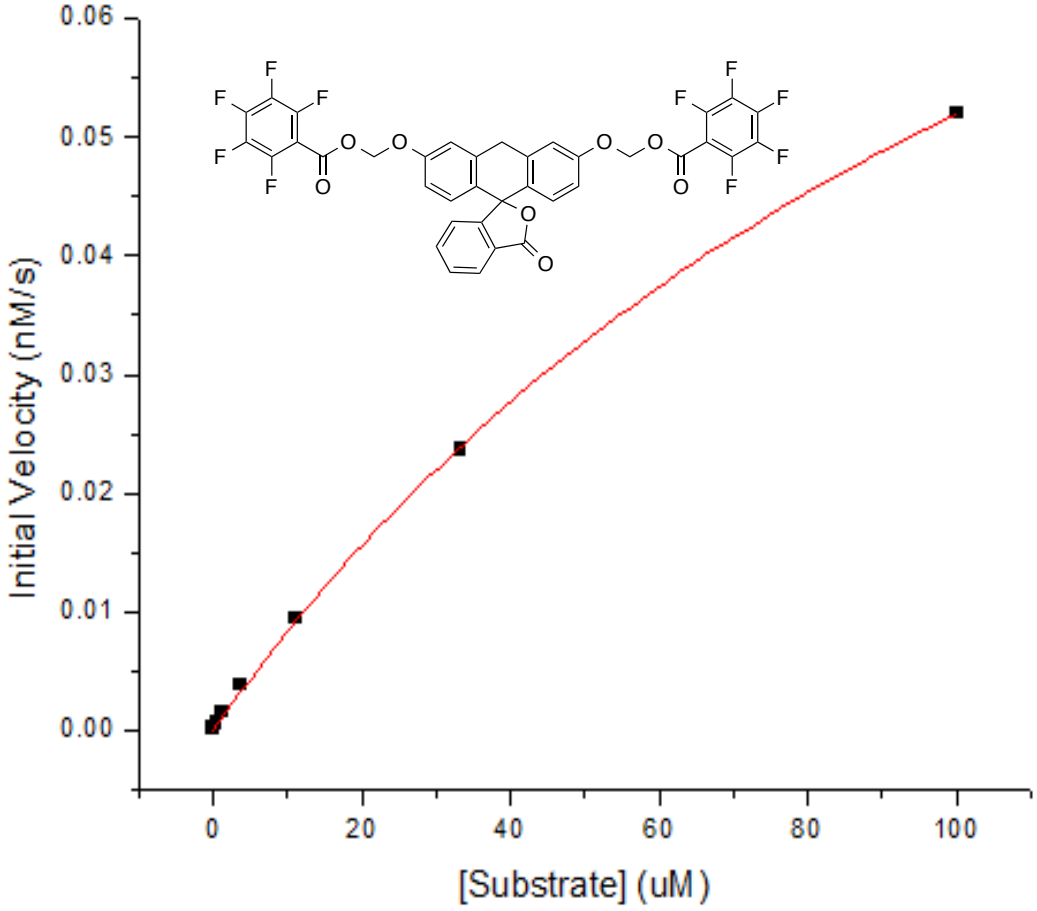

Chi^2/DoF	1.4701E-7	
R^2	0.99962	
V_{MAX}	0.00007	±0.00003
K_M (M)	0.125	±0.005
K_{cat} (s^{-1})	0.00042	±2E-5

Fluorescein di(pentafluorophenacetoxymethyl ether) FPME
Substrate #14

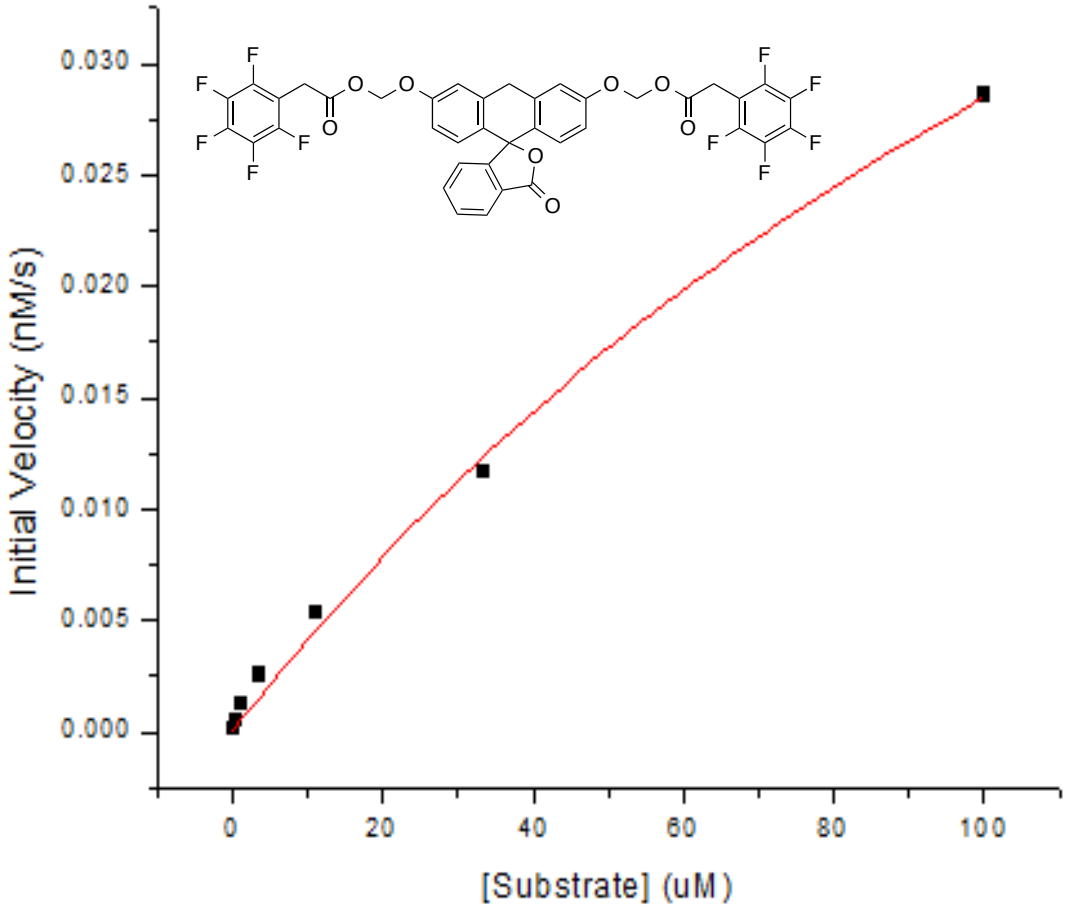

Chi^2/DoF	4.5365E-7	
R^2	0.99597	
V_{MAX}	0.08	±0.02
K_M (M)	188	±49
K_{cat} (s^{-1})	0.00023	±4E-5

Fluorescein di(trifluoropropionoxymethyl ether) TFME
Substrate #15

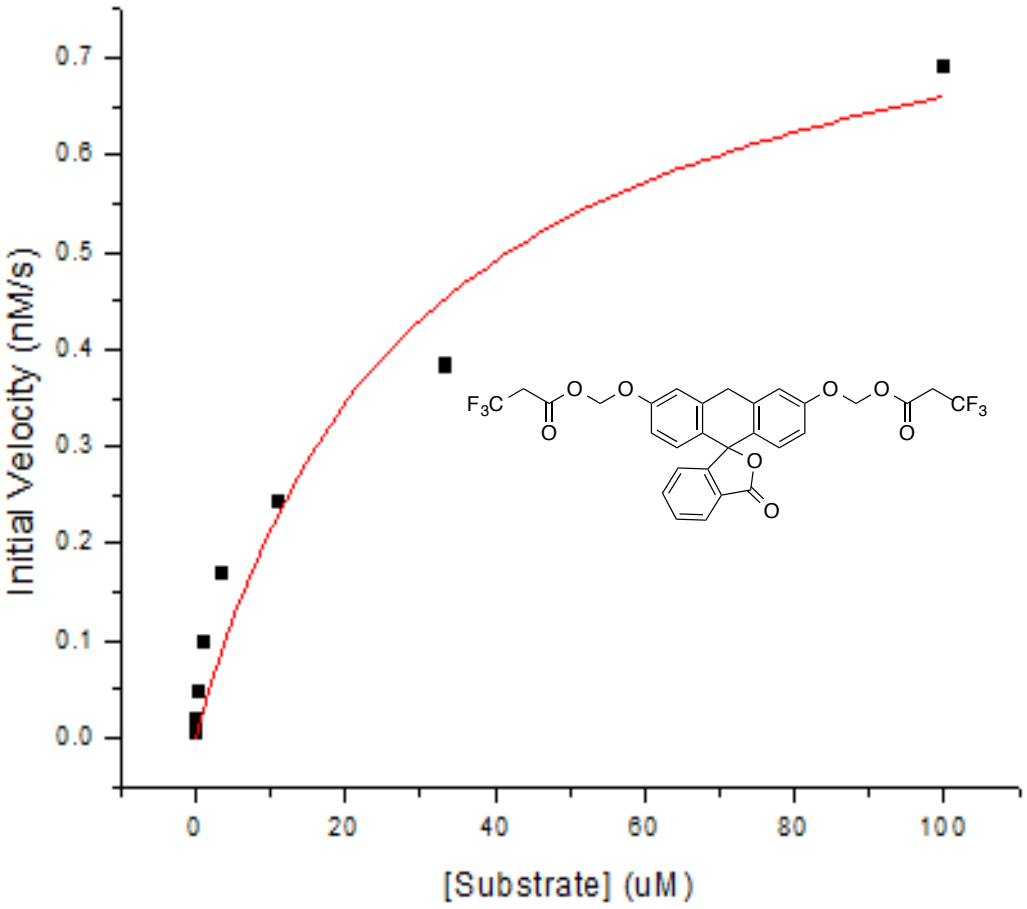

Chi²/DoF	0.00276	
R²	0.95644	
V_{MAX}	0.9	±0.12
K_M (M)	30	±11
K_{cat} (s^{-1})	0.0024	±3E-4